ARL 65-203
OCTOBER 1965

Aerospace Research Laboratories

SUPERSONIC WIND TUNNEL TESTS OF WAVY-WALLED CYLINDERS

WILLIAM J. ANDERSON
THERMO-MECHANICS RESEARCH LABORATORY

OFFICE OF AEROSPACE RESEARCH
United States Air Force

ARL 65-203

SUPERSONIC WIND TUNNEL TESTS OF WAVY-WALLED CYLINDERS

WILLIAM J. ANDERSON

THERMO-MECHANICS RESEARCH LABORATORY

OCTOBER 1965

Project 7063
Task 7063-02

AEROSPACE RESEARCH LABORATORIES
OFFICE OF AEROSPACE RESEARCH
UNITED STATES AIR FORCE
WRIGHT-PATTERSON AIR FORCE BASE, OHIO

FOREWORD

This research was carried out by the Thermo-Mechanics Laboratory, Aerospace Research Laboratories. It was a part of Project 7063, "Research in Flight Mechanics" under Task 7063-02, "Research in Structures". The wind tunnel testing was done at the Supersonic Gasdynamics Facility located at Wright-Patterson Air Force Base and operated by the Air Force Research and Technology Division. Tests were run intermittently from February 1964 to April 1964.

A great deal of assistance was given on this project by Lt. Dale Herman and Mr. Harold Zimmerman. Their help is sincerely appreciated. The wind tunnel models were made by General Electric at their Large Jet Engine Dept., Evandale Plant, Cincinnati, Ohio. The difficult job of installing pressure tubes in the models was ably carried out by Mr. Don Linder and Mr. Frantz Hebbeler. Special thanks are due to Mr. Joe Nenni, Mr. Howard White and the operating crews of the Supersonic Gasdynamics Facility. Mr. Ralph Lickert cheerfully took care of the photographic work.

Theoretical curves shown in Figures 21 and 25 were supplied by Mr. Lee Saunders of the Marshall Space Flight Center, Huntsville, Alabama.

ABSTRACT

The primary objective of this experiment was to provide pressure measurements for use in flutter calculations. Wavy-walled cylinders were wind tunnel tested at Mach 3.0 and 4.62. The walls of the cylinders were rigid, with a sinusoidal deflection pattern machined in the outer surface. The waves extended in both the axial and circumferential direction. Flow was directed along the cylinder axis. Static pressures were measured at the wavy surface of each cylinder. The pressure perturbations proved to be smaller in amplitude than predicted by inviscid aerodynamic theories. The pressure distribution also had a small phase shift downstream. The tests are helpful in studying viscous flow effects on the pressures. A direct comparison with an existing idealized boundary layer theory was impossible, however, because of the choice of wave height on the model. Boundary layer separation occurred under some conditions. Separation was observed in the form of a small bubble lying behind a wave, particularly in regions where the boundary layer was laminar. Oil film studies were made by using a thin film of oil on the surface. When exposed to ultraviolet light, the oil film fluoresced, revealing the stream line pattern. Photographs of the oil film patterns and a number of Schlieren pictures are presented. Some details are given pertaining to the model fabrication because of the new manufacturing processes used.

TABLE OF CONTENTS

LIST OF FIGURES

LIST OF FIGURES

NOTATION

A_l	Amplitude factor in pressure expression, Equation 2
E	Probable error in least squares fit to experimental data
ℓ	Axial wave length
M	Mach number
N	Total number of static pressure taps on a given wave, Eqn. 4
n	Circumferential wave number
p	Static pressure of fluid
$\bar{p}(x, r, \theta, t)$	Perturbation pressure in fluid due to wall deflection
p*	Constant used in least squares fit to experimental data
$\bar{p}_i$	Static pressure perturbation measured at the i th tap, Eqn. 4
P_t	Total pressure
R	Cylinder radius
r	Radial coordinate
t	Time
U	Fluid velocity
$w(x, \theta, t)$	Radial deflection of cylinder surface
w_o	Constant
x	Axial coordinate
δ	Idealized boundary layer thickness of Reference 21
θ	Angular coordinate
ψ_l	Phase angle in pressure expression, Equation 2
ρ	Fluid density

BLANK PAGE

I. INTRODUCTION

A study of the flutter of a structure requires a precise knowledge of the fluid forces involved. One flutter problem of current interest is a type of panel flutter which occurs on cylindrical shells. This is a wave-like instability in the thin skin of a circular cylinder exposed to flow along the cylinder axis. A typical application would be the flutter of the outer skin of a missile rising through the atmosphere. Cylinder flutter has been observed only in supersonic flow.

Several types of wave motion at the surface of a cylinder have been theoretically studied[1-12]. These theories consider cylinders exposed to supersonic flow as shown in Fig. 1. Some of these references consider the finite length cylinder and some consider the infinitely long cylinder. As the cylinder deflects, perturbation pressures are generated at the cylinder surface. The spatial distribution of these pressures is of particular interest here.

A number of studies in recent years have indicated that there may be a significant boundary layer effect on an oscillating wall. Experimental work by Lock and Fung[13] led to the conclusion that the boundary layer was stabilizing for the flutter of flat panels in the transonic region. This experimental observation was confirmed by McClure[14] in a study of two-dimensional wavy walls at supersonic Mach numbers less than 2. A theory by Miles[15] for short wave length traveling waves on an infinitely long cylinder showed that the boundary layer did not change the flutter boundary significantly but reduced the instability by an order of magnitude. Other boundary layer studies dealing primarily with instabilities within the boundary layer have been carried out by Kramer[16], Benjamin[17] and Landahl[18].

Manuscript released 9 June 1965 by the author for publication as an ARL Technical Documentary Report.

The present effort stems directly from the cylinder flutter tests by Stearman, Fung and Lock[19] and the theory of Anderson and Fung[20, 21]. The experiments by Stearman, Fung and Lock were carried out in 1961 and 1962. These tests at Mach 2.5 to 3.5 raised some questions about the accuracy of existing aerodynamic theories. As a result, an idealized boundary layer theory was developed to determine whether or not the boundary layer might have an effect on cylinder flutter.

The idealized boundary layer theory was admittedly crude, yet some of its features were interesting. In this theory, the boundary layer was replaced by a uniform layer of subsonic gas. The thin layer of subsonic gas was found to have a striking effect on the pressures predicted for an oscillating cylinder, particularly for modes with many circumferential waves. It was found that pressure amplitudes were attenuated and significant phase shift in the pressure could occur.

A decision was made to continue this cylinder flutter work at the Aerospace Research Laboratories. It was decided to make static pressure measurements on rigid, wavy-walled cylinders at the higher Mach numbers. Pressure measurements on an oscillating wall would have been preferable, but are beyond the state of the art at the present time (for the complicated wave forms of interest here). The stationary wall can provide a great amount of information for the present.

It was the purpose of the tests described here to measure the static pressure perturbations on a cylindrical shell with a surface deflection:

$$w(x, \theta) = w_o \cos n\theta \sin(2\pi x/\ell). \tag{1}$$

Linear aerodynamic theories predict a resulting surface pressure of the form

$$\bar{p}(x, \theta) = \frac{w_o}{R} \frac{\rho U^2}{M} \frac{2\pi R}{\ell} A_1 \cos(n\theta) \cos\left(\frac{2\pi x}{\ell} + \psi_1\right) \tag{2}$$

where A_1 is an amplitude factor and Ψ_1 is a spatial phase angle. In particular, linear piston theory gives $A_1 = 1.0$ and $\Psi_1 = 0$. The pressures measured in these tests proved to be out of the linear range. The pressures, however, did vary in an approximately sinusoidal fashion. Equation (2) is of some value in assigning an amplitude A_1 and a phase Ψ_1 to typify each pressure distribution. (A "least squares" fit to the experimental data was used.)

The wind tunnel tests were carried out at the Supersonic Gasdynamics Facility located at Wright-Patterson Air Force Base, Ohio. This is a closed circuit, continuously operating tunnel with a test section two feet by two feet in cross section. Mach numbers 3.0 and 4.62 were used, with a variation in total pressure from approximately 1/4 to 2 atmospheres.

II. MODEL DESIGN

The wind tunnel models are shown in Figs. 2, 3, and 4. They were made in three interchangeable cylindrical sections including a nose, a wavy-wall section and a tail. A total of two noses, three wavy-wall sections and one tail were made. The wavy-wall sections differed only in the number of circumferential waves, n = 0, 10, and 20. It is convenient to designate the models #0, #10, and #20 according to the circumferential wave number. Only the aerodynamic forces on the external surface of the model were of interest. The flow was ducted through the model to prevent wind tunnel "blockage."

The wave pattern machined in the wavy-wall test section was sinusoidal in both the axial and circumferential directions. The equation of the radial surface deflection (measured from the mean radius) was

$$w(x, \theta) = w_o \cos n\theta \sin\left(\frac{2\pi x}{\ell}\right) \qquad (n = 0,\ 10,\ 20)$$

where the wave half-amplitude w_o = 0.040 inch and the wavelength $\ell = \pi/2$ inch. The mean outside diameter of the wavy-wall cylinder was 10.000 inches. Each model had a total of 12 waves in the axial direction. Brass plate 1/2 inch thick was rolled and welded into the cylindrical form needed for the models.

It was desired to build the models with waves as shallow as possible, in order to prevent separation. A conflicting requirement was that the waves had to be deep enough to cause perturbation pressures which could be read on a manometer board. (The boundary layer theory predicted low pressures.) It was also necessary to have the wave height sufficiently large that the machine tolerance would be small compared to wave height. As a result, a compromise height of 0.080 inch peak-to-peak was chosen.

Machining the models proved to be an ambitious project. They were made at General Electric's Large Jet Engine Department, Cincinnati, Ohio.

Models #10 and #20 were made on a 3 axis, numerically controlled, contour milling machine. This was a numeric Keller machine controlled by a computer using magnetic tape instructions. Four degrees of freedom (relative motion between model and cutter head) were used to make the pieces. A 2" diameter ball cutter was used for both models. The model design called for a tolerance of $\pm$ 0.0005" on the wavy surface. The computer instructions were generated for this tolerance; however, additional error crept in because of cutter wear, deflection of the model and wear in model positioning devices.

Wavy wall #0 was made in a different way, on a computer-controlled lathe. Some error was incurred because the tailstock of the lathe was not precisely set. The wave pattern was accurately machined, but the mean diameter of the model increased from 10.003" at the nose to 10.009" at the tail.

The surface finish left by this machine process is different from that in conventional machining processes. The surface is rough because the cutter moves in discrete increments designed only to keep the tolerance within the specified limit. Figure 5 shows a close-up picture of wavy wall #20. A portion of the surface has been polished and a portion has been left as machined.

The sketches in Fig. 6 show how the model was machined and polished. A cross-section normal to the cylinder axis is shown. The machine instructions were programmed in such a way that the machined surface was to lie within the two dashed curves shown in Fig. 6a. The resulting machined surface appeared as in Fig. 6b, with cusps lying between the paths taken by the cutter. These cusps were polished down by hand using a fine grade of emery paper. Measurements on a sample piece indicated that the final tolerance of the surface was improved by this polishing. Care was taken not to polish out the bottom of the tool marks because these marks formed a reference surface.

Measurements of the surface profile were taken after the models were completed. The models were mounted on a jig borer and depth readings were

taken with a dial gage equipped with an electrical continuity meter (to accurately determine contact between indicator shaft and model). Measurements taken in the axial direction were used in a computer program for a least squares sine wave fit. In this way, it was found that the surfaces were accurate to a root mean square error of 0.0007" with an error in phase shift of 2^{o} or less for each wave. Some marks on the bodies were as deep as 0.003". The phase error was corrected out of the static pressure measurements from the tests.

Static pressure orifices were installed in the model before the wavy wall was machined. In this way, the ends of the pressure tubes were machined flush with the contour of the surface. The bore of each tube was positioned perpendicular to the cylinder axis rather than perpendicular to the local slope. Each of the three models had 5 waves instrumented in the axial direction. Waves #1, 4 and 7 were instrumented with 9 pressure taps each and waves #9 and 11 with 5 taps each. These pressure taps were distributed along axial lines at $\theta=0^{o}$ and $\theta=90^{o}$ (maximum deflections occur along these lines). The use of 9 taps proved to be sufficient to define the pressure pattern on one wave. Five taps were too few, especially when it was suspected that a separation bubble was present behind one of the "hills" on the model. In addition to these taps, models #10 and #20 were instrumented with 9 orifices extending in the circumferential direction and defining one circumferential wave.

The pressure taps were made from 1/16" O.D. and 1/32" I.D. brass tube. This tube was connected to 1/8" O.D. brass tubing which led outside the tunnel to a silicone manometer board. Lag time for the pressure readings was on the order of 2 minutes at the lowest tunnel operating pressures.

One thermocouple was placed in the wall of each model to record wall temperatures. The thermocouple was press fitted into a hole bored from the interior of the cylinder to within 0.040" of the outer surface.

Two noses were used on the models (see Figs. 3 and 4). Nose #1 was made of steel and #2 was made of brass . Both had sharp leading edges and were 10" in length. Nose #1 had an external taper of 2^{o} extending over the forward 3" of the nose. It was felt that the external taper on the nose would prevent separation behind the sharp leading edge in case the model was slightly misaligned. The outside surface of nose #2 was cylindrical; it had no taper. In the tests, there appeared to be no measurable different in the perturbation pressures on the body due to the different noses. Nose #1 (with external taper) was used almost exclusively in the tests.

The tail section was made of carbon steel and was designed to slip over a sting mount in the wind tunnel. The model mounted rigidly to the sting.

Model #20 is shown installed in the tunnel in Fig. 7. It is seen to be cantilevered from the rear. It could be pitched easily to align it in the flow. Yaw corrections proved unnecessary and pitch corrections were much less than a degree. A boundary layer trip is shown on this model. A layer of carborundum grit one inch wide was used in an effort to fix the boundary layer transition on the nose and to thicken the boundary layer. At Mach 4.62, #60 grit was used; at Mach 3.0, #120 grit was used. The attempt was not successful; the trip appeared to have no effect at either Mach number.

A total pressure probe was used to measure boundary layer velocity profiles (Fig. 8). Theprobe could be traversed through a distance of 1.7" normal to the surface. A ball and socket joint allowed proper positioning. The orifice used was 0.016" I.D. and 0.020" O.D. at the tip. Pressures were read on a U-tube manometer equipped with both silicone and mercury legs. Liquid heights could be read to 0.001". Lag time for this probe system was approximately 5 minutes for the slowest case (when close to the body at low tunnel dynamic pressure).

The idealized boundary layer theory of Reference 21 can be used to predict the perturbation pressures on the surface of the models. Fig. 9 shows the pressures predicted for the models at Mach 3.0. The boundary layer thickness δ characterizes the boundary layer, but is unspecified in the theory.

The idealized boundary layer theory, in order to apply to the experiment, required that $2w_o \ll \delta \ll \ell$. Upon entering the tests, it was assumed that the quantity δ was associated with the displacement boundary layer thickness. This would make $0.080'' \ll \delta \ll 1.57''$ a realizable inequality. As the tests progressed, it became apparent that the quantity δ was more likely of the order of the thickness of the subsonic portion of the boundary layer. Thus the idealized model did not strictly apply to the experiment.

The wave heights proved to be larger than desired. First of all, from the order of magnitude estimates above, it would have been better to have wave heights small compared to the subsonic portion of the boundary layer. Secondly, the pressure perturbations would have been smaller. It was found that nonlinear pressure distributions resulted, as well as boundary layer separation under some conditions.

III. TEST TECHNIQUES

Each of the models was tested in a similar manner. The model was mounted in the tunnel and the static pressure tubes connected and leak checked. The total pressure probe was positioned over the specific wave to be studied. Flow was established. The model alignment in the tunnel was checked by reading static pressures on top, bottom and sides of the nose.

Testing was done at total pressures P_t from 500 to 3500 psf in increments of 500 psf. Total temperatures were varied from 80° to 110°. The corresponding Reynolds number R_e ranged from 0.55×10^6 to 3.1×10^6 per foot. Schlieren pictures were taken at each P_t setting.

Velocity profiles in the boundary layer were taken under several conditions. Each profile took approximately 30 minutes because of the relatively high lag time and because of the detail of the velocity profile.

In order to study possible boundary layer separation effects, oil film studies were made. A thin coat of 40 weight motor oil was rubbed on parts of the wavy-wall surface. Under ultraviolet light, the oil luminesced, revealing the streamline pattern about the body. This procedure was especially valuable in a qualitative way for detecting separation. The presence of separation bubbles at some R_e was noted using this technique, and was confirmed from pressure measurements and boundary layer velocity profiles.

IV. RESULTS

In studying the results, it is best to first consider the general flow conditions on the model. The static pressure results are of primary interest, but will be discussed later.

A. GENERAL FLOW CONDITIONS

Static pressure recovery on nose #1 is shown in Figure 10. The tunnel static pressure was measured at an orifice in the side wall of the test section, slightly ahead of the model nose. In all but two cases, the pressure on the nose at a point 8 inches to the rear of the leading edge was within 1% of the tunnel static pressure. Two cases measured showed a recovery to within only 2% of tunnel static pressure. It can be concluded that the static pressure of the flow had essentially returned to the upstream value before entering the wavy-wall section.

Fig. 11 is an oil film study of the flow over several waves of model #10. This type of flow occurred over portions of the bodies at Mach 3.0 when at higher total pressures (Reynolds number/foot). Flow patterns such as this corresponded to acceptable surface static pressure readings. The amount of flow angularity shown is striking; the flow situation is definitely three-dimensional.

Velocity profiles in the boundary layer were taken at Mach 4.62. Fig. 12 shows two profiles taken on the 7th and 9th waves. These profiles were calculated from total pressure readings. It was assumed that static pressure and total temperature were constant through the boundary layer. Total temperature was taken to be the adiabatic wall temperature as measured by a thermocouple at the model surface. The effect of weak shock waves emanating from upstream "hills" can be seen.

B. SEPARATION

Under some conditions, separation occurred on the model in the form of separation bubbles behind the hills. Gross separation, where flow might leave the body and not reattach, was never observed. Separation proved to occur more seriously at Mach 4.62 than at Mach 3.0. It almost always occurred where the boundary layer was laminar and sometimes occurred in the turbulent boundary layer at the rear of the body.

The separation bubble on model #0 was in the form of a closed ring extending around the body and lying behind a hill. (See Fig. 13). On model #10, there were often two separation bubbles symmetrically spaced behind the hills. Figures 14 and 15 show this pattern. It could not be determined from the available instrumentation whether these bubbles were fixed in time or whether they indicate a time average of a vortex shedding phenomenon. Model #20 also experienced this type of separation (Fig. 16). There appears to be a single separation bubble behind the hills on this model. This may be due to the shorter circumferential wave length causing an overlapping of the two bubbles which were distinct on model #10.

Further comments on separation can be made from a study of static pressures at the model surface. More information on separation is given in the next two sections.

C. SCHLIEREN PICTURES

Schlieren pictures were taken at every data point. A number of pictures are presented here for general interest. These pictures are similar to those obtained by Czarnecki and Monta[27] for their axisymmetric wavy wall models.

One important thing to note is the change in character of the shock pattern and boundary layer as flow progresses down the model. This is undoubtedly associated with boundary layer transition, but detailed comments are

not possible because of the limited amount of measurement done in the boundary layer.

The Schlierens for model #10 at Mach 3. 0 are of interest. At P_t = 500 psf, the flow is laminar down the length of the model. The boundary layer appears to shield the hills from the main stream. At P_t = 1000 psf, transition appears to occur in the vicinity of the 7th wave. In the turbulent boundary layer region, the shock waves appear to originate at a point closer to the body (probably because the profile is "fuller"). The shock waves are stronger in the turbulent boundary layer region. As P_t is raised to 1500 and then to 2500 psf, the transition point moves upstream until it is near the 2nd wave.

It was observed early in the tests that the static pressure distribution always indicated flow separation behind the first wave. This was at first attributed to a leading edge effect (due perhaps to the discontinuity in slope at the start of the wavy wall section). The Schlierens, however, revealed a correlation between laminar boundary layer and separation for these models. The first wave was always in the laminar region and hence always separated.

There is a flaw in the optical system which causes a bright spot on the fifth wave in each picture. This is not a part of the flow pattern.

A nonlinear solution for flow over axisymmetric wavy-walled cylinders has been developed by Sims, Saunders and Platzer[23]. The method of characteristics was used in this solution. Boundary conditions are applied at the precise position of the wavy surface rather than at the mean radius of the cylinder. The solution includes the effects of the shock waves and of the finite leading edge. Boundary layer effects are neglected. The resulting solution can be used to predict the position of the shock waves on the model and the pressure distribution. The shock

wave pattern for model #0 at Mach 3. 0 is given in Figure 21.

D. STATIC PRESSURES

Typical static pressures at the model surface are shown in Figures 22, 23 and 24 in terms of a pressure coefficient $C_p = \overline{p}/(\frac{1}{2}\gamma pM^2)$. In Figure 22, it is clear that the flow has separated on waves #1 and #7. The pressure distributions on waves #4 and #11 indicate attached flow.

Figure 25 shows an interesting theoretical solution for the static pressures on model #0 at Mach number 3. 0. This is the method of characteristics solution[23] discussed in the previous section. The theory yields larger positive pressure perturbations than negative perturbations, with almost no phase shift (at this particular wave length). The peak-to-peak variation in pressure is approximately the same as given by the linear potential solution of Leonard and Hedgepeth. The measured perturbations are smaller than the theoretical values, but it is apparent that the positive pressure perturbations are greater in magnitude than the negative.

In order to discuss the pressure data in a convenient way, without presenting it all in graphical form, it is necessary to resort to an oversimplification of the pressure wave form. From the nonlinear solution, it is realized that the measured pressures should not be expected to be sinusoidal. On the other hand, the experimental data can be fitted with a sine wave to give an approximate measure of pressure amplitude and phase shift. The following expression was used:

$$p(x) = p^* + \frac{w_o}{R}\,\frac{\rho U^2}{M}\,\frac{2\pi R}{\ell}\,A_1 \cos\left(\frac{2\pi x}{\ell} + \psi_1\right)$$

A "least squares" fit was used to determine the parameters p^*, A_1 and ψ_1.

The sine fit of the data is also useful to make a crude distinction between separated and unseparated flow. A normalized error associated with the fit can be defined:

$$E = \frac{1}{A_1}\sqrt{\frac{\sum_{i=1}^{N}\left[p(x_i) - \overline{p}_i\right]^2}{N-3}} \qquad (4)$$

where $p(x_i)$ is the theoretical value and $\overline{p}_i$ is the experimental value. This quantity will be used as a measure of the "goodness of fit." The factor (N - 3) is used to provide an unbiased estimate of the variation. It takes this

value because there are three independent variables in the fit. This factor is necessary in order to make a meaningful comparison between data taken on waves with 5 orifices and those with 9 orifices.

Typical values of E are given in parentheses under each wave in Figures 22, 23 and 24. From observations of plotted pressure data, the following scheme was used to define separation:

$0 \leq E \leq 0.125$	unseparated
$0.125 < E < 0.150$	doubtful data
$0.150 \leq E$	separated

One result of this approach is given in Fig. 26. It is seen that almost no usable data were obtained in the laminar boundary layer region. Usable data generally occurred in the turbulent boundary layer region immediately downstream of the transition point. It is possible that the transition to a turbulent boundary layer causes the separation point to move back on the wave, similar to separation on a sphere in subsonic flow. On these sine waves, however, the separation point might be moved downstream far enough to cause separation to disappear entirely on a given wave. Fig. 26 indicates that separation also occurs on the body some distance downstream from transition.

The pressure results will now be summarized. Figures 27, 28, 29, and 30 show all of the pressure data from the tests. For model #0, there were no data for $E < 1.25$; however, data for $.125 \leq E \leq .152$ are given in Fig. 27.

Whether compared with linear piston theory, the potential theory of Leonard and Hedgepeth or the nonlinear solution by Saunders, Sims and Platzer, the experimental results show an attenuation in pressure and a negative phase shift. There appears to be little difference in the pressures measured on the three models. At Mach 3.0, pressures are from 50% to 75% of potential

values. At Mach 4.62, pressures fall off to 27% to 37% of potential values, although these results are of dubious value. The phase shift is approximately -10°.

A full interpretation of these data cannot be made at this time. The results do confirm one prediction of the nonlinear method of characteristics solution for model #0 - - the positive pressure perturbations are larger than the negative. This is apparent from Fig. 25.

The effects of separation are difficult to distinguish in these results. If the separation on the upstream hills was actually in the form of a shedding vortex, then there may have been some effect on downstream pressures.

Some additional comments are made concerning separation on the models by Herman in his M.S. Thesis carried out at the Air Force Institute of Technology[24].

E. BRIEF DISCUSSION OF WORK BY OTHERS

Two other supersonic tests of wavy-walls have been run. McClure[14] tested two-dimensional wavy-walled plates at Mach 1.405. Czarnecki and Monta[22] tested axisymmetric cylinder models at Mach 1.6 and 2.0.

McClure measured a pressure attenuation and a substantial phase shift upstream. These effects were attributed to the boundary layer. A theory was developed to account for boundary layer effects at Mach numbers below 2. It successfully predicts the transonic boundary layer effect and indicates that this effect should diminish as Mach number approaches 2. McClure's measurements show a qualitative effect similar to that predicted by the idealized boundary layer of Anderson & Fung. On the other hand, McClure's theory suggests that there should be little boundary layer effect on axisymmetric cylinders at higher Mach numbers. The extension of McClure's results to the axisymmetric cylinders at high Mach numbers must be done with caution, however.

In Czarnecki and Monta's tests, the pressures approach the potential values, although some cases appear attenuated. The phase shift was not given explicitly. The plotted data shows a small phase shift upstream.

It is difficult at this time to make direct comparisons between the present measurements, the experiments of McClure, the experiments of Czarnecki and Monta, and the idealized boundary layer theory. The tests were different geometrically and in Mach number tested. None of the tests appear to have had wave heights small enough to allow the idealized theory to apply.

V. DISCUSSION OF RESULTS

A number of experimental observations have been made. A full interpretation of the pressure results is not possible at this time. This is due to the uncertainty in the role played by boundary layer separation. Separation bubbles were always present on the leading wave of the model. These bubbles may have affected the unseparated region (downstream) in a way which is difficult to identify. All pressure data showing a suspicious "jump" or irregularity were thrown out using a statistical approach. The remaining pressure data exhibit the properties discussed in the following five paragraphs.

The pressure perturbations were sufficiently strong to lie outside the range of linear theory. Nonsinusoidal pressure distributions resulted. Positive pressure perturbations were larger in magnitude than the negative perturbations. This agrees qualitatively with the nonlinear method of characteristics solution for model #0.

The pressure coefficients A_1 were smaller than predicted by linear and nonlinear inviscid theory. Also, A_1 increased with increasing Reynolds number/foot (decreasing boundary layer thickness). These effects qualitatively agree with the idealized boundary layer theory and are not consistent with inviscid theory.

The pressure coefficient A_1 was approximately the same for models #0, 10 and 20 at Mach 3. This conflicts with the idealized boundary layer theory but agrees with Leonard and Hedgepeth's potential solution.

A small negative (downstream) phase shift was measured on all three models. The phase angle ψ_1 did not vary with Reynolds number. Inaccuracy of the model surface did not cause this phase shift. The model was measured

accurately after manufacturing. Error due to machine inaccuracy and tap location was less than 2^{o} for each wave. The data were corrected for this error, which was small compared to the average ψ_1 reading (approximately -10^{o}). No existing theories predict a negative phase shift.

The experiment does not confirm the idealized boundary layer theory. This theory predicted an attenuation in pressure amplitude, a phase shift upstream, and a substantial difference in pressures on models #0, 10 and 20. Only the pressure attenuation was observed in the experiment. Upon entering the tests, there was an uncertainty in interpreting the quantity δ characterizing the boundary layer thickness in the idealized theory. It was felt that δ would be associated with the displacement boundary layer thickness. This has been shown not to be so. It now appears necessary to associate δ with the thickness of the subsonic portion of the boundary layer. In the present tests, this would mean that the amplitude of the waves was too high for the idealized boundary layer theory to apply. As a result, this test is felt to be inconclusive as a check on the idealized boundary layer theory. If future tests are to be made, shallower waves should be used.

As mentioned above, boundary layer separation occurred on certain areas of the models. Separation bubbles on model #0 were in the form of closed rings extending around the body and lying behind the waves. Small separation bubbles appeared on models #10 and 20. There was no case where the flow completely separated from the bodies, i. e., where the flow might detach and not reattach at a point downstream.

Separation was more severe at Mach 4.62 than at Mach 3.0. Also, separation was more severe for model #0 than for models #10 and 20. Separation

usually occurred where the boundary layer was laminar. In particular, for model #10 at Mach 3.0, a correlation was found between boundary layer transition and boundary layer separation. Separation bubbles always appeared in the region of laminar boundary layer. Immediately downstream of boundary layer transition on this model, unseparated flow existed for 4 or 5 waves. Separation bubbles again appeared at the rear of the model.

The fact that transition to a turbulent boundary layer prevented separation may be analogous to the case of flow over a sphere. The turbulent boundary layer does not separate as easily as the laminar, and the separation point moves downstream. On a wavy-wall model, the separation point can be moved far enough back on a given wave to make separation disappear entirely.

In the future, it may be of interest to test models with longer axial wave lengths. Linearized supersonic potential theory predicts a phase shift upstream approaching 90° when axial wave length is long compared to circumferential wave length.

VI. REFERENCES

1. Leonard, R. W. and Hedgepeth, J. M.: "On Panel Flutter and Divergence of Infinitely Long Thin-Walled Circular Cylinders," NACA Report 1302, 1957.

2. Stepanov, R. D.: "On the Flutter of Cylindrical Shells and Panels Moving in a Flow of Gas," Prikladnaia Matematika i Mekhanika, 21, 5, 1957; also NASA TM 1438, 1958.

3. Miles, J. W.: "Supersonic Panel Flutter of a Cylindrical Shell," I-Journal of Aeronautical Sciences, 24, 2, pp 107-118, February 1957. II-Journal of Aeronautical Sciences 25, 5, pp 312-316 May, 1958.

4. Shulman, Y.: "Vibration and Flutter of Cylindrical and Conical Shells," AFOSR TR 59-776, Massachusetts Institute of Technology, June, 1959.

5. Voss, H. M.: "The Effect of an External Supersonic Flow on the Vibration Characteristics of Thin Cylindrical Shells, "Journal of Aerospace Sciences, 28, 12, Dec. 1961.

6. Krumhaar, H.: "Supersonic Flutter of a Cylindrical Shell of Finite Length in an Axisymmetric Mode," AFOSR 1574, October, 1961.

7. Holt, M. and Strack, S. L.: "Supersonic Panel Flutter of a Cylindrical Shell of Finite Length," Journal of Aerospace Sciences, 28, 3, p 197, March, 1961.

8. Dzygadlo, Z.: "Linearized Supersonic Flow Past a Vibrating Surface of a Body of Revolution," Proceedings of Vibration Problems, Polish Academy of Sciences, 2, 3, 1961.

9. Dzygadlo, Z.: "Self Excited Vibration of a Cylindrical Shell of Finite Length in Supersonic Flow," Proceedings of Vibration Problems, Polish Academy of Sciences, 3, 1, 1963.

10. Dzygadlo, Z.: "The Problem of Aeroelasticity of a Cylindrical Panel and a Plate Strip Taking into Consideration the Transversal Coupling" Proceedings of Vibration Problems, Polish Academy of Sciences 5, 2, 1964.

11. Platzer, M. P.: "On the Calculation of Linearized Subsonic and Supersonic Flow Over Oscillating Bodies," Ph. D. Dissertation, Technical University of Vienna, February, 1964.

12. Des Clers, B. and Chang, C.: "On Some Problems in Linearized Axisymmetric Flow," Journal of Aerospace Sciences, 18, 2, pp 127-138, February, 1951.

13. Lock, M. H. and Fung, Y. C.: "Comparative Experimental and Theoretical Studies of the Flutter of Flat Panels in a Low Supersonic Flow," AFOSR TN 670, May, 1961.

14. McClure, J.D.: "On Perturbed Boundary Layer Flows," Mass. Inst. of Tech., Fluid Dynamics Research Laboratory, Report No. 62-2, June, 1962.

15. Miles, J.W.: "On Panel Flutter in the Presence of a Boundary Layer," Journal of Aerospace Sciences, 26, 2, pp 81-93, February, 1959.

16. Kramer, M.O.: "Boundary-Layer Stabilization by Distributed Damping," Journal of American Society of Naval Engineers, 72, 1960.

17. Benjamin, T.B.: "Effects on a Flexible Boundary on Hydrodynamic Stability," Journal of Fluid Mechanics 9, 1960.

18. Landahl, M.T.: "On the Stability of a Laminar Incompressible Boundary Layer Over a Flexible Surface," Journal of Fluid Mechanics 13, 1962.

19. Stearman, R.O., Lock, M.H., and Fung, Y.C.: "Ames Tests on the Flutter of Cylindrical Shells," California Institute of Technology Report SM 62-37, December 1962.

20. Anderson, W.J. and Fung, Y.C.: The Effect of an Idealized Boundary Layer on Flutter of Cylindrical Shells in Supersonic Flow," California Institute of Technology SM 62-49, December, 1962.

21. Anderson, W.J.: "Oscillatory Pressures in an Idealized Boundary Layer with an Application to the Panel Flutter of Cylindrical Shells," Paper to be presented at AIAA Symposium on Structural Dynamics and Aeroelasticity, Boston, Mass, August, 1965.

22. Czarnecki, K.R. and Monta, W.J., "Pressure Distribution and Wave Drag Due to Two-Dimensional Fabrication-Type Surface Roughness on an Ogive Cylinder at Mach Numbers of 1.61 and 2.01, " NASA TN D-835, 1961.

23. Sims, Saunders and Platzer, Marshall Space Flight Center, Huntsville, Alabama, Unpublished Communication.

24. Herman, D.J.: "An Experimental Study of Boundary-Layer Separation on a Family of Wavy-Walled Cylinders," M.S. Thesis, Air Force Institute of Technology, June, 1964.

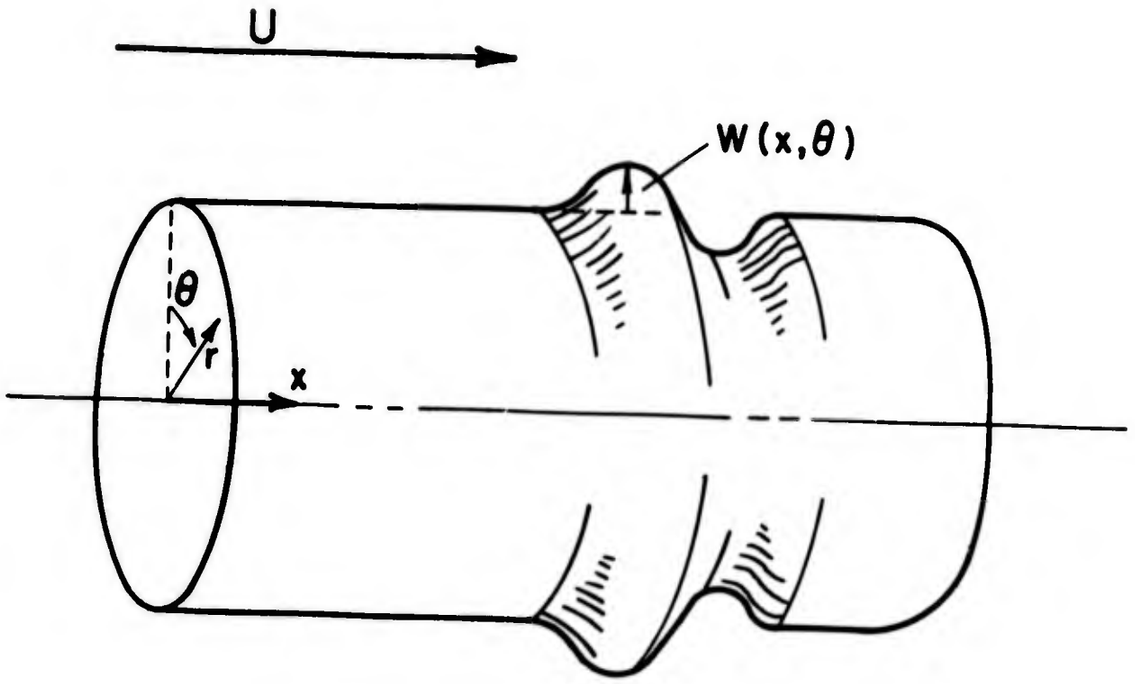

Fig. 1 Coordinate System

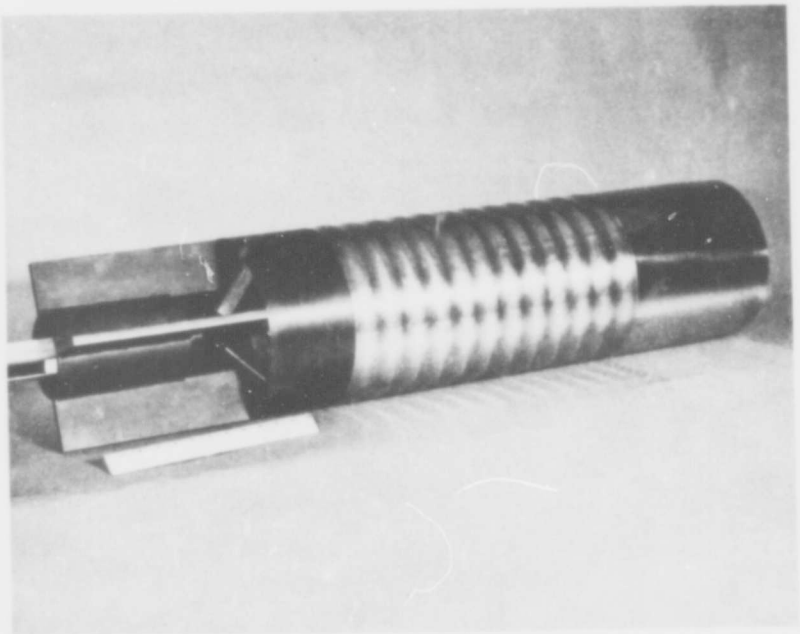

Fig. 2 Model #0, Nose #1.

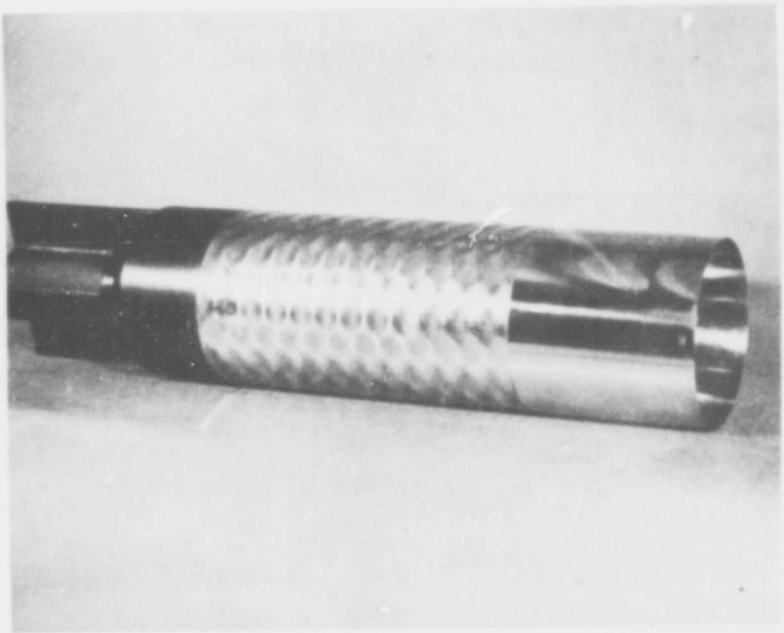

Fig. 3 Model #10, Nose #1.

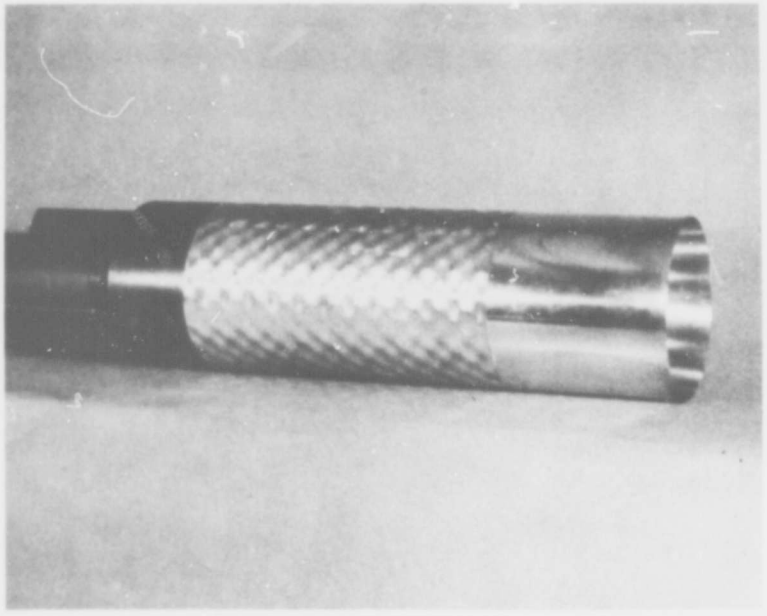

Fig. 4 Model #20, Nose #2.

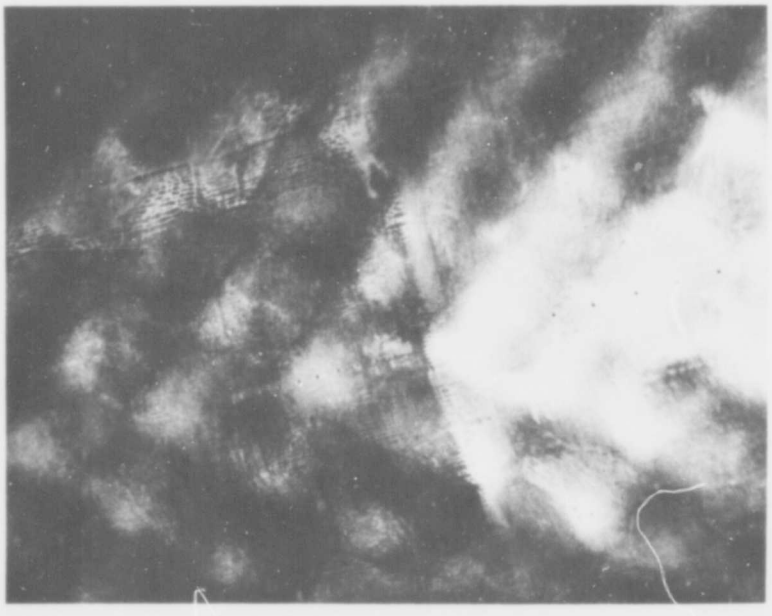

Fig. 5 Closeup of Surface on Model #20.

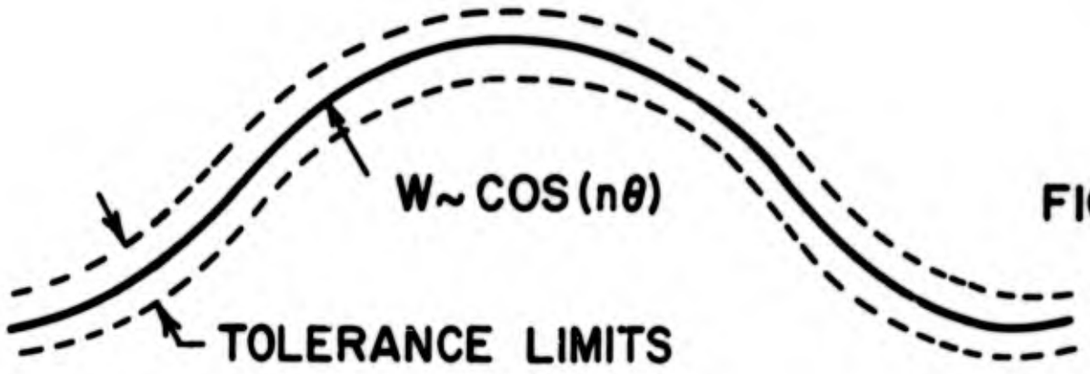

FIG. 6a

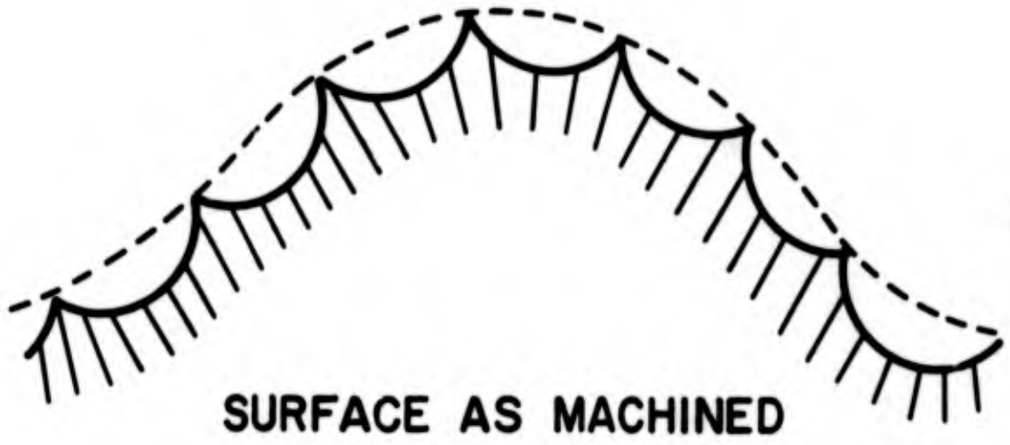

FIG. 6b

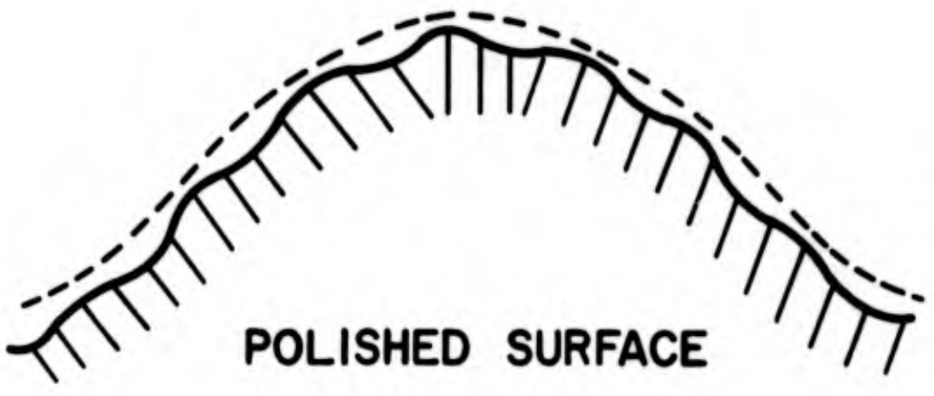

FIG. 6c

Fig. 6 Surface Finish on Models (Not to scale).

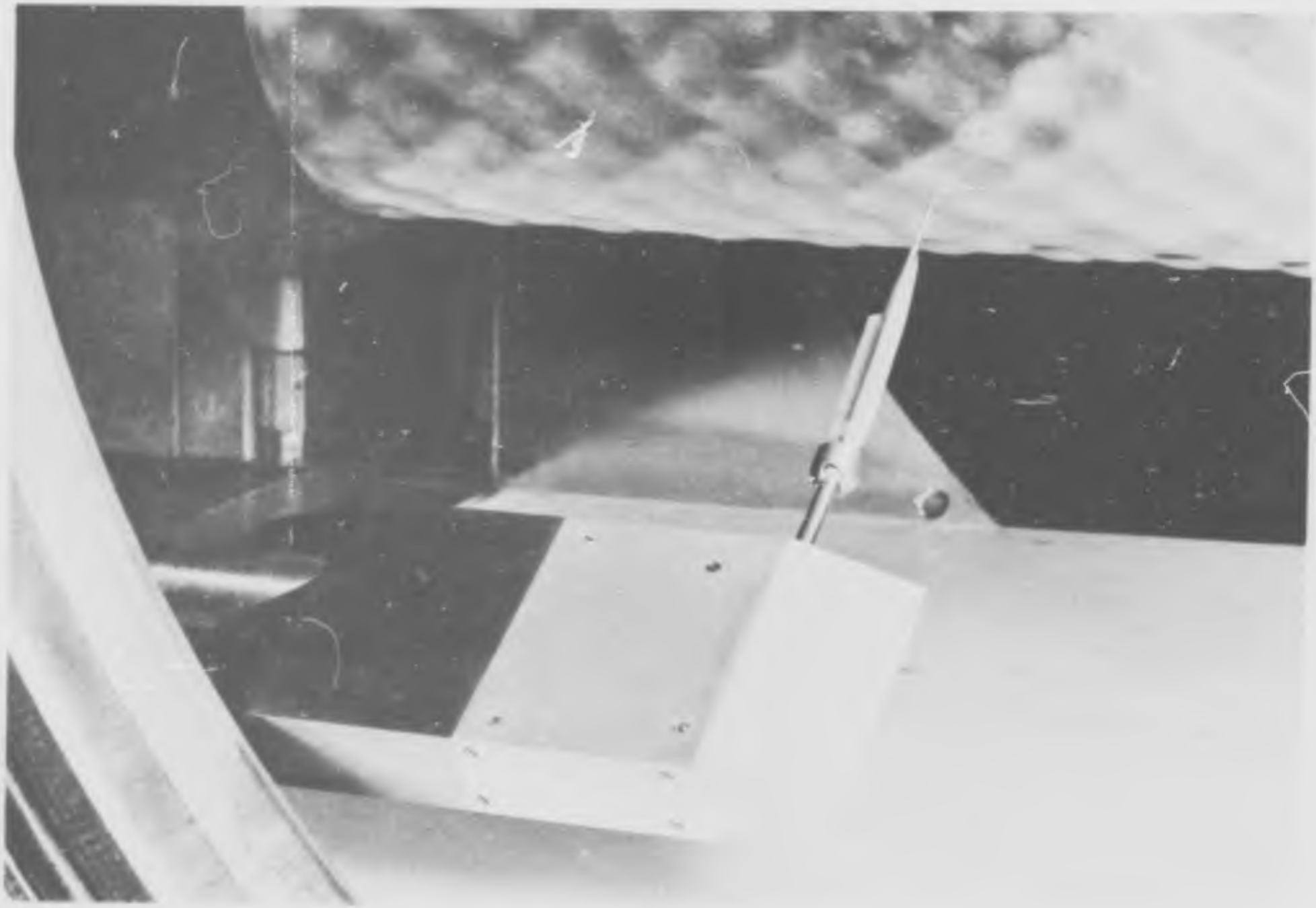

Fig. 8 Total Pressure Probe

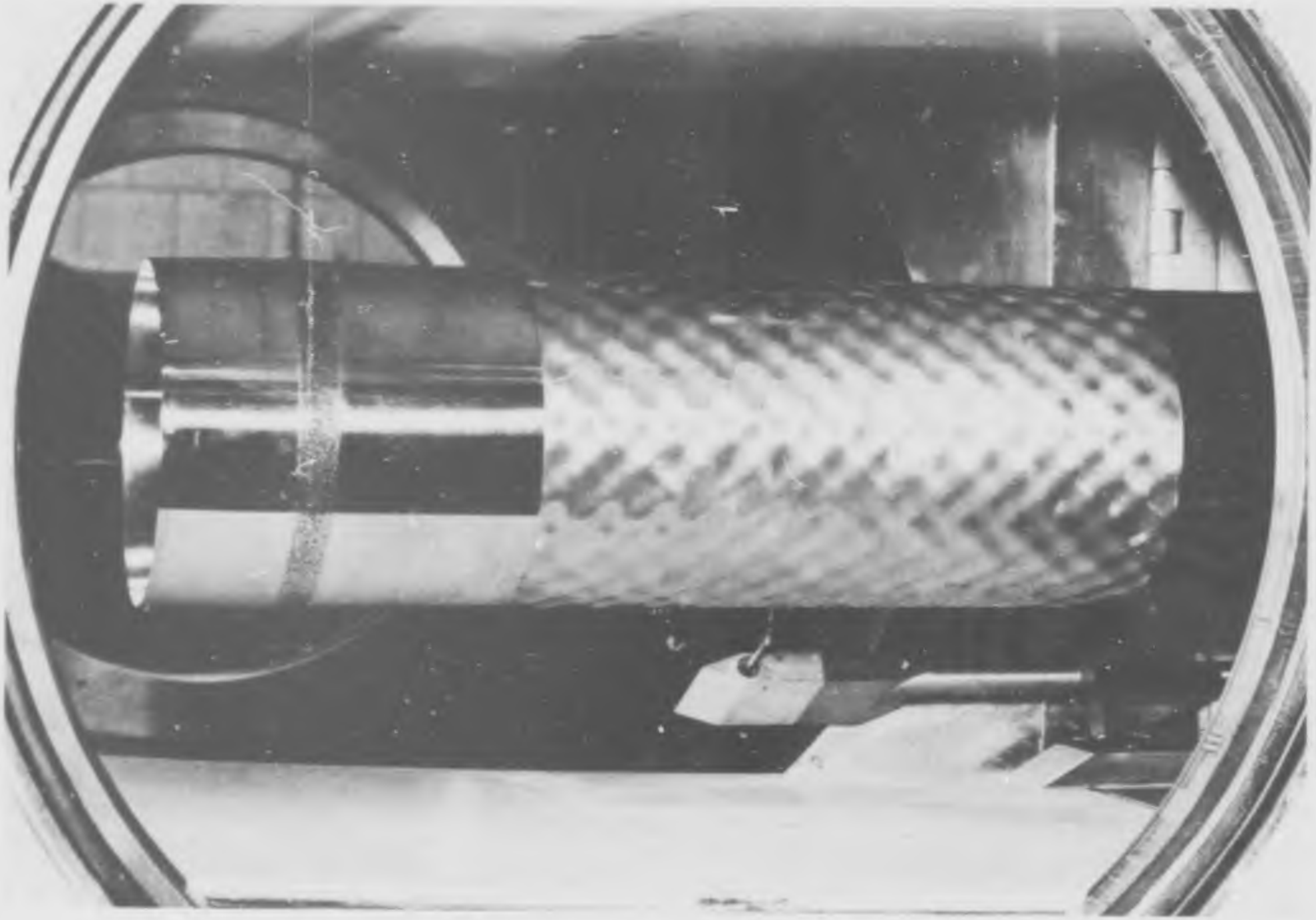

Fig. 7 Model #20 Installed in Wind Tunnel

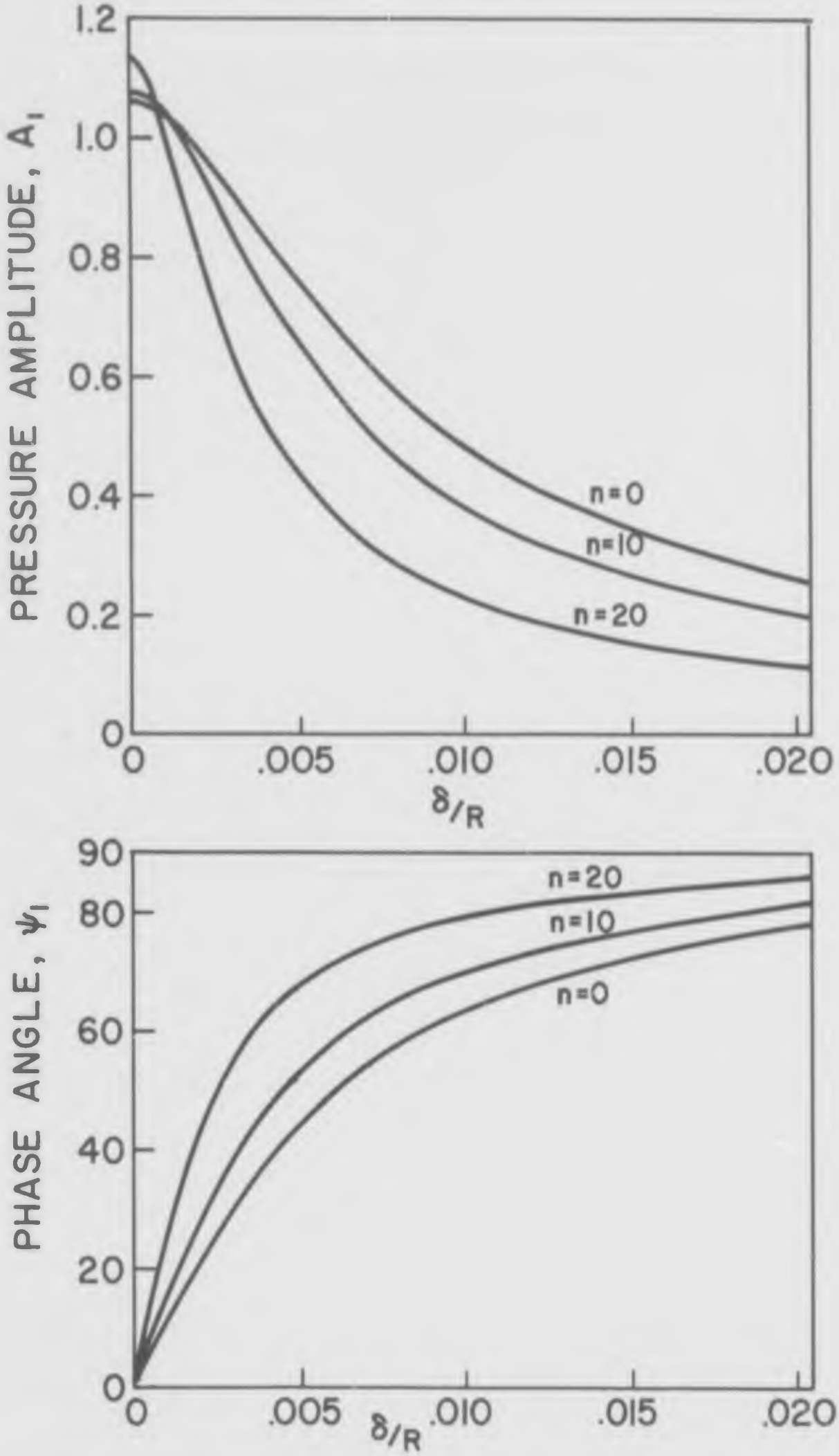

Fig. 9 Predicted Static Pressures at Mach 3.0 Idealized Boundary Layer Theory[21].

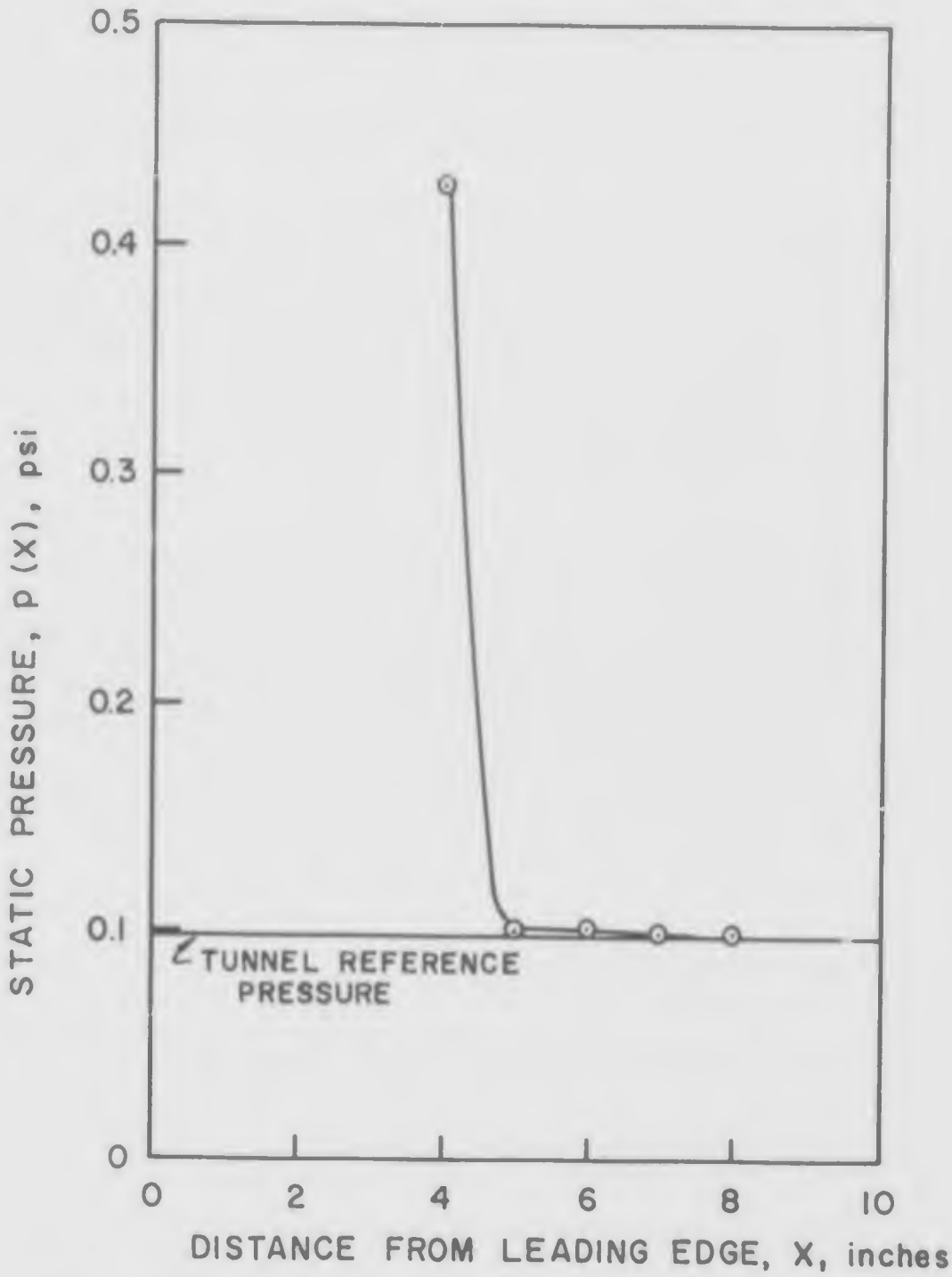

Fig. 10 Static Pressure Recovery on Nose #1. (M = 3.0, P_t = 500 psf., Boundary Layer Trip at $3.5 \leq x \leq 4.5$)

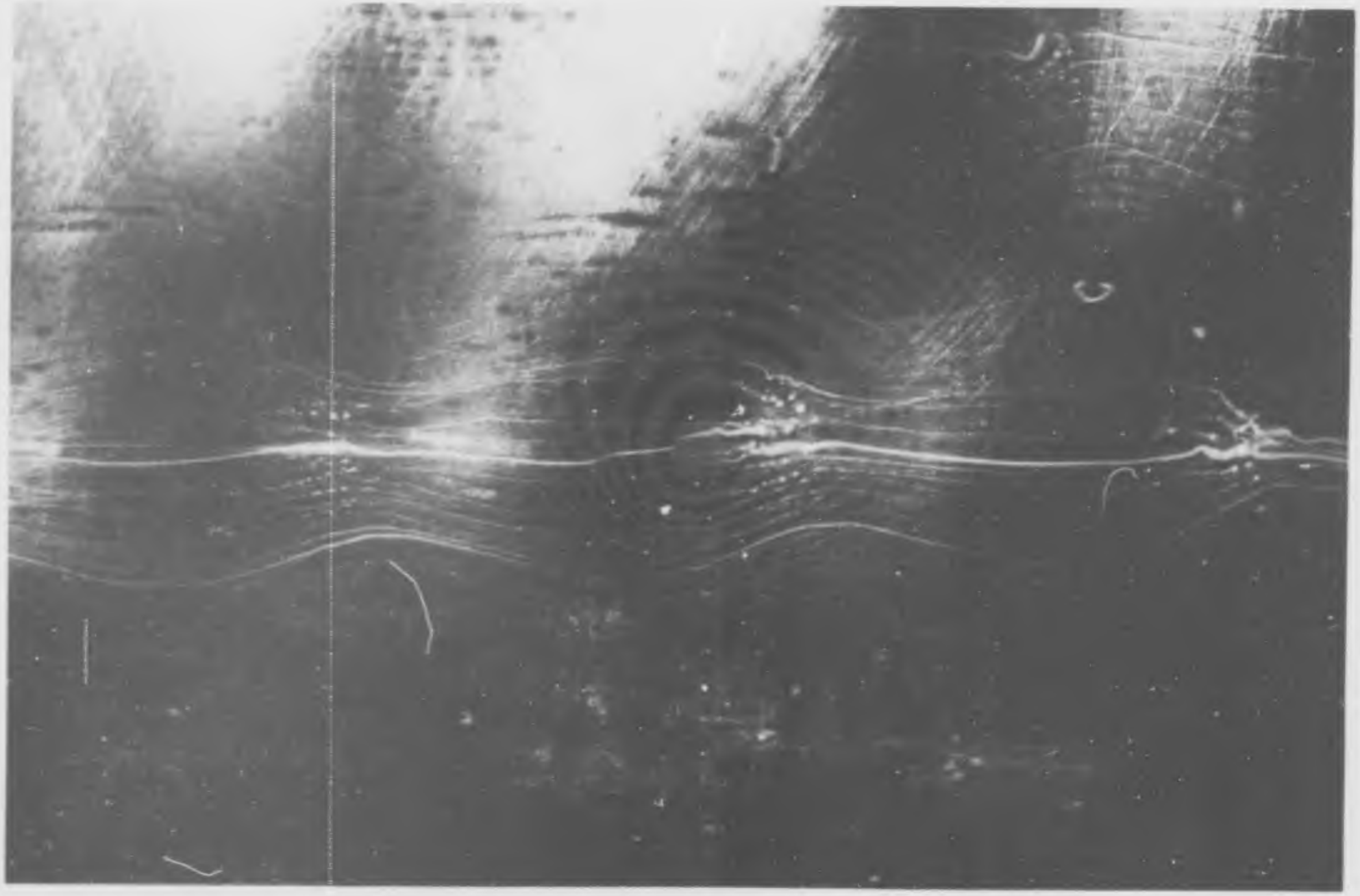

Fig. 11 Oil Film Study. Model #10 at Mach 3.0

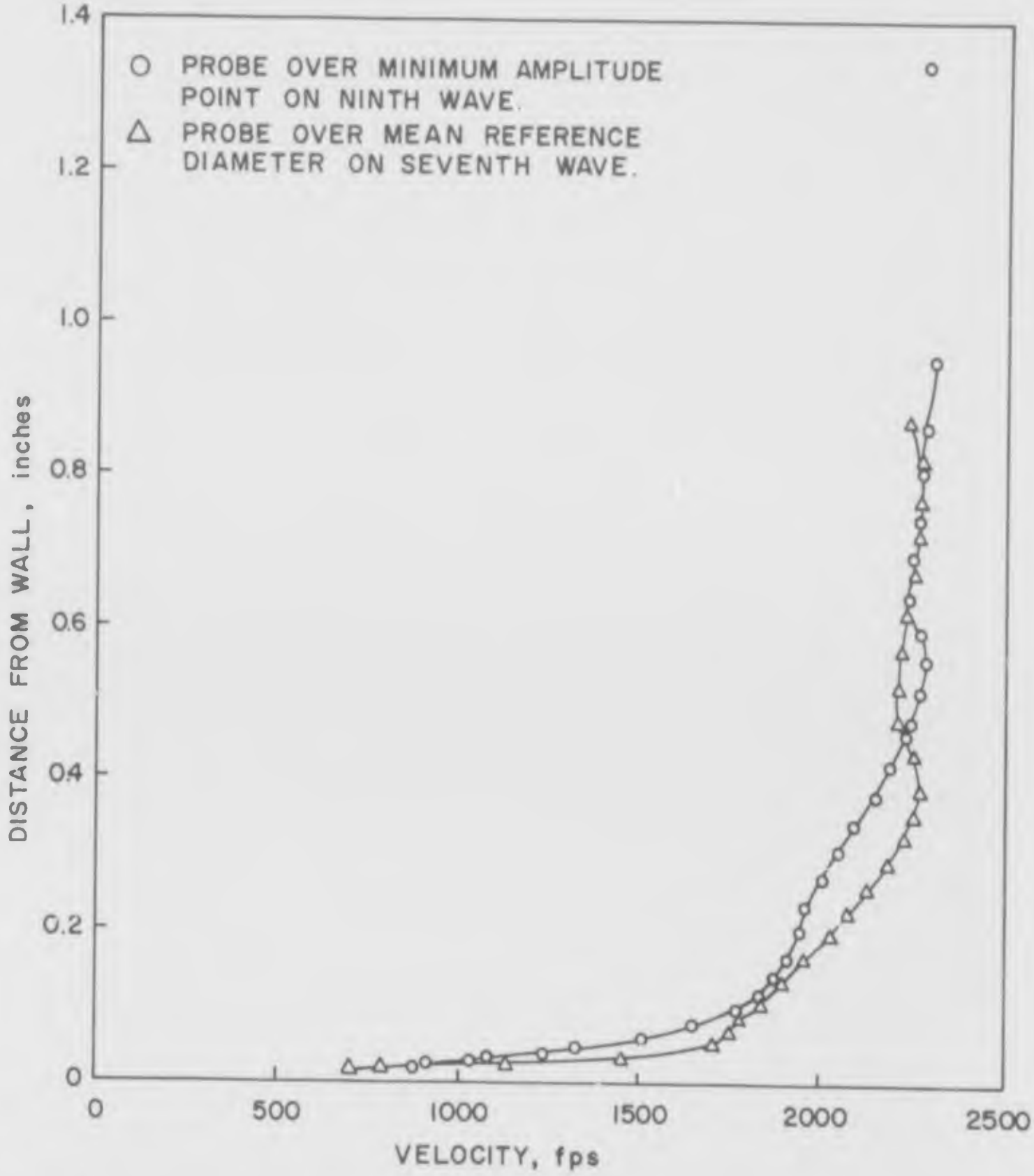

Fig. 12 Velocity Profiles Measured on Model #0 at Mach 4.62. (Static Pressure and Total Pressure Assumed Constant Through Boundary Layer Thickness).

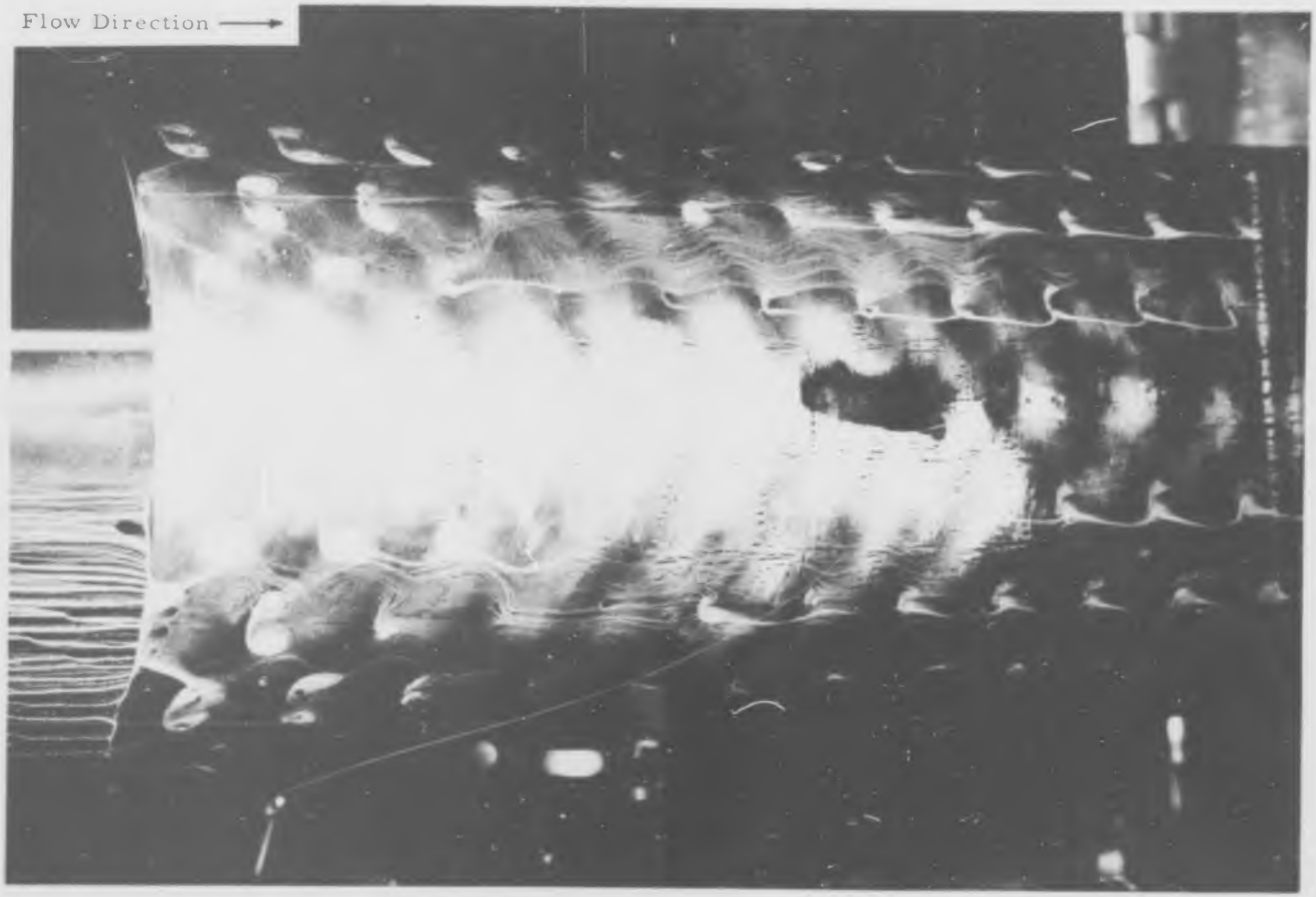

Fig. 14 Separated Flow on Model #10. (M = 3.0, P_t = 500 psf.)

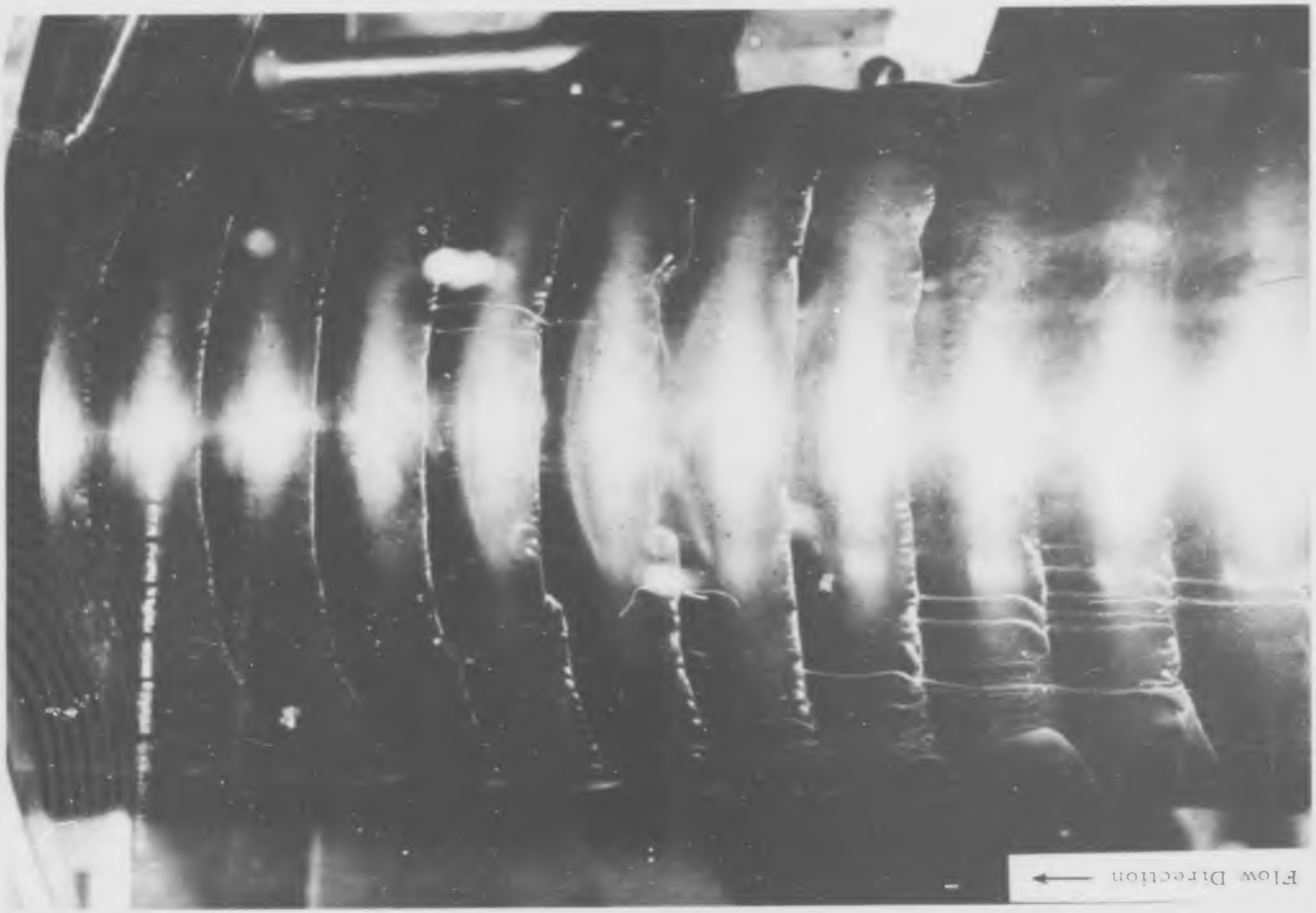

Fig. 13 Separated Flow on Model #0. ($M = 4.62$, $P_t = 2000$ psf.)

Fig. 15 Separated Flow on Model #10. ($M = 4.62$, $P_t = 4000$ psf.)

Fig. 16 Separated Flow on Model #20. (M = 4.62, P_t = 4000 psf.)

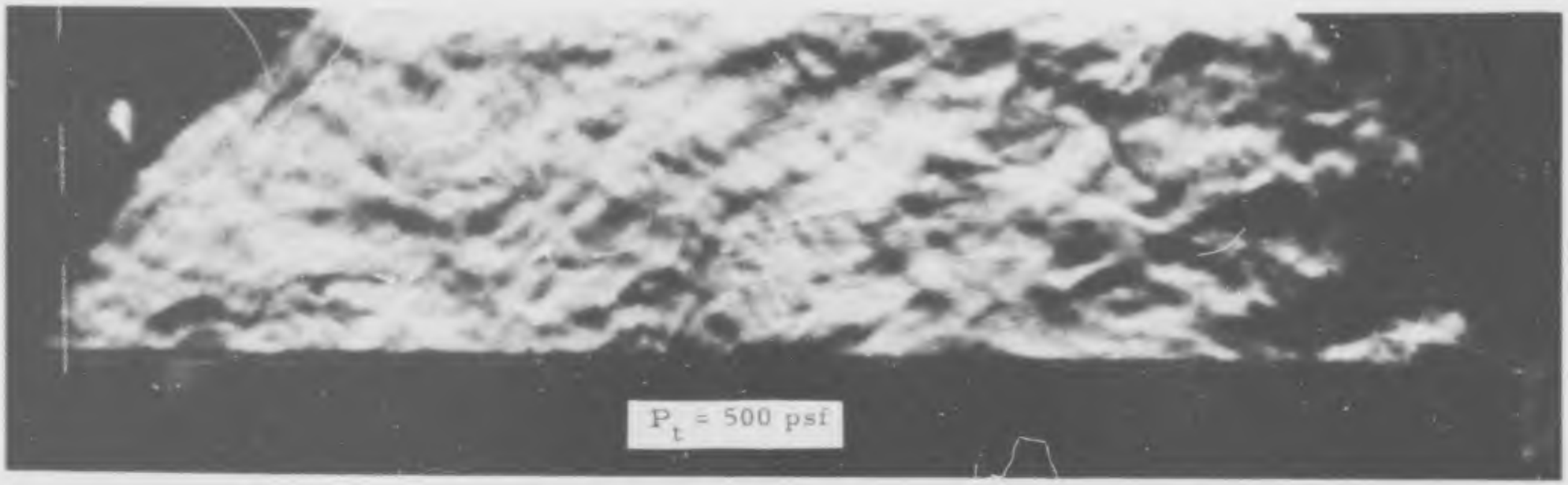

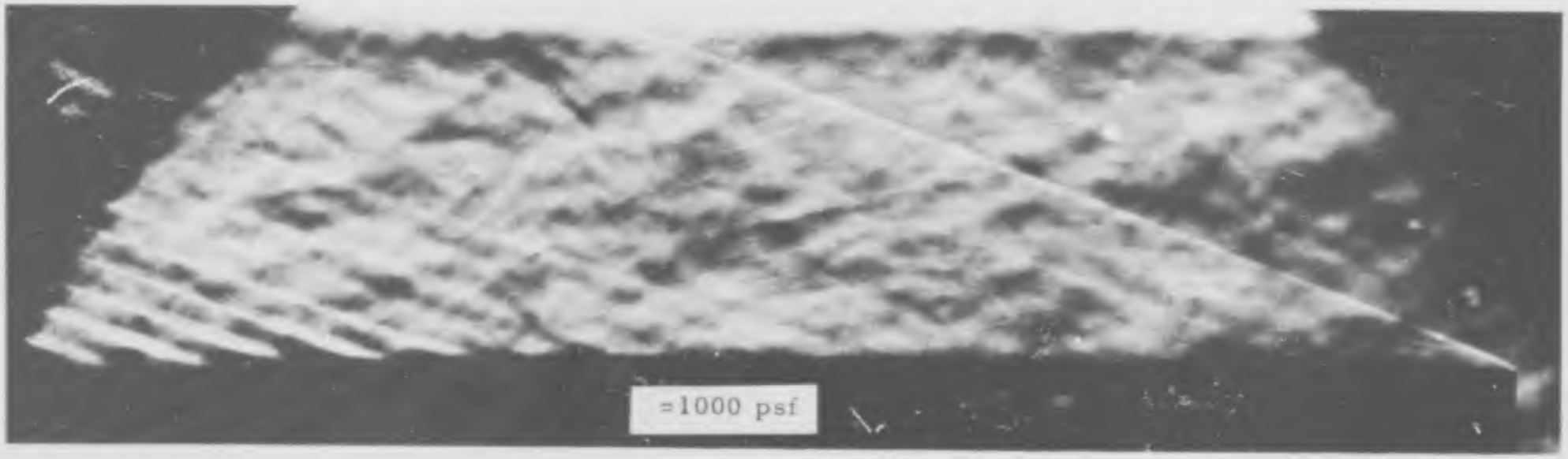

Fig. 18a Shock Pattern on Model #10 at Mach 3.0

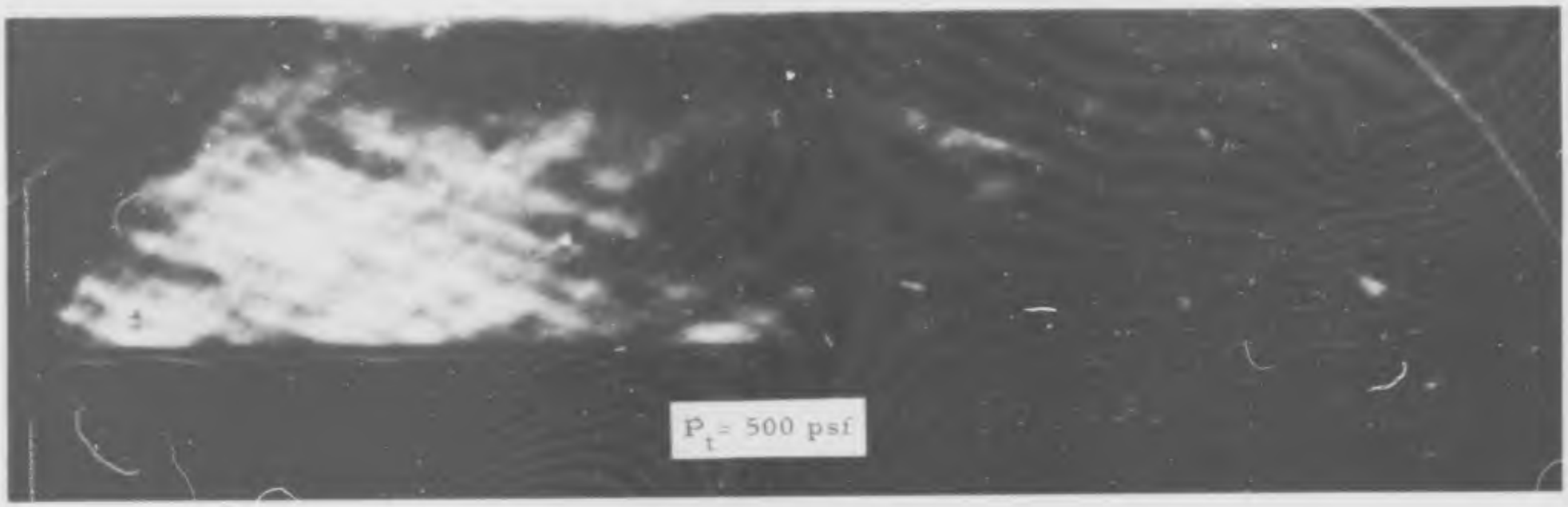

Fig. 17 Shock Pattern on Model #0 at Mach 3.0.

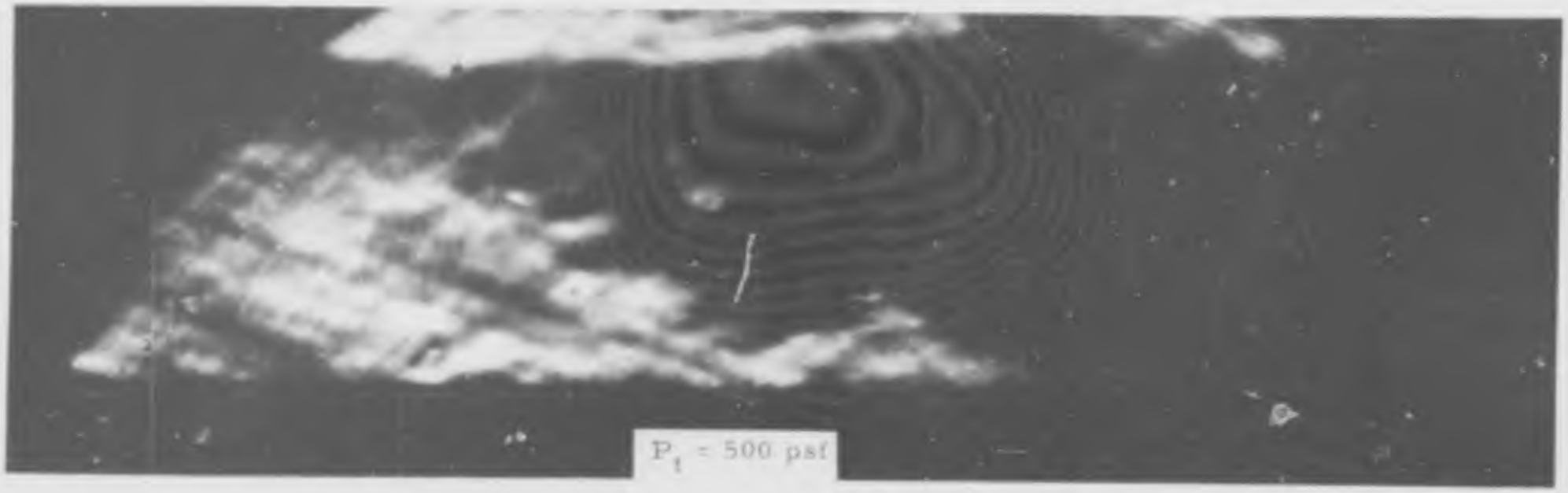

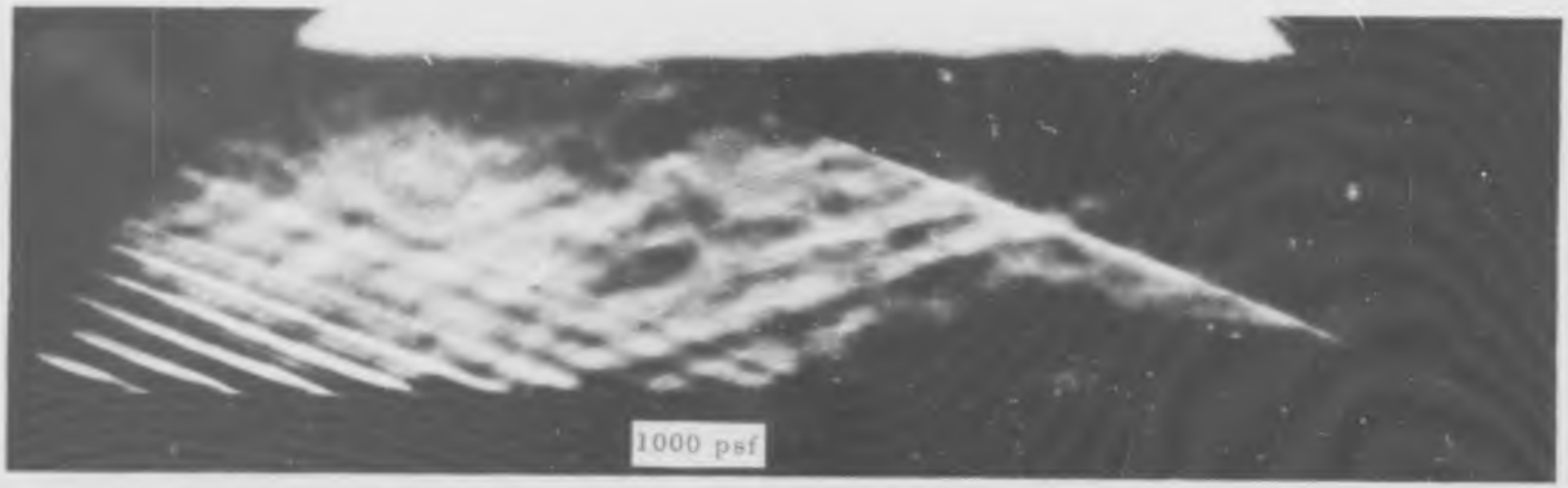

Fig. 19a Shock Pattern on Model #20 at Mach 3.0

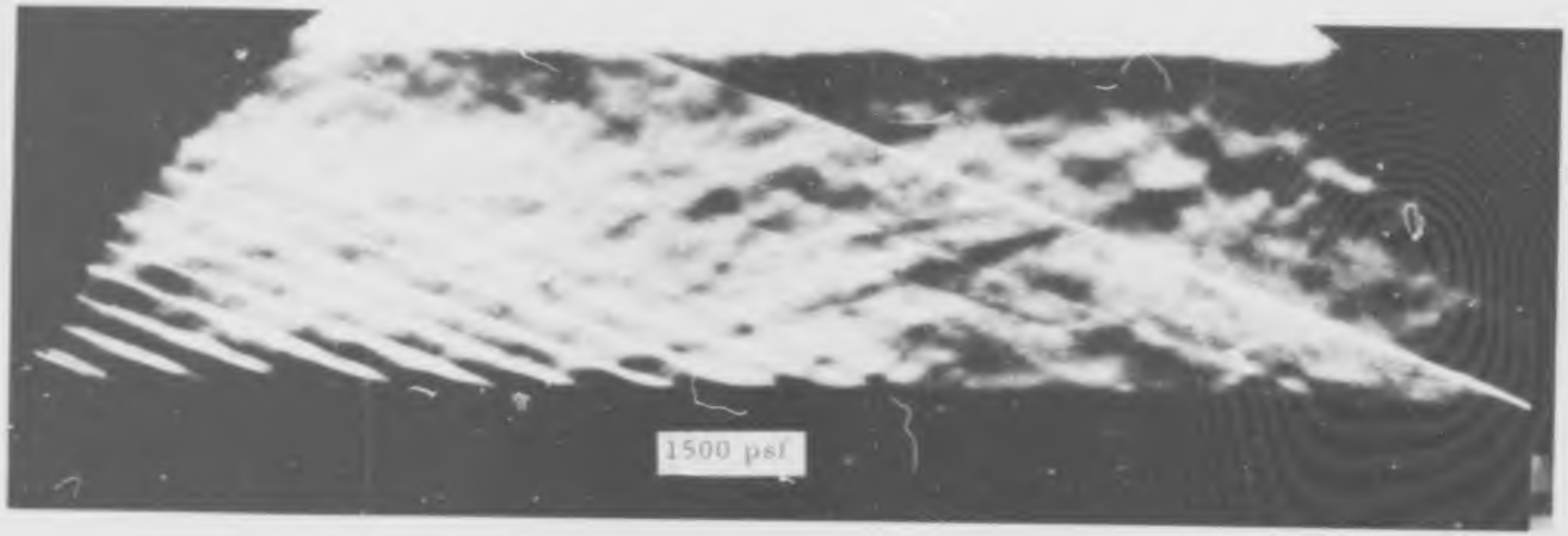

Fig. 18b Shock Pattern on Model #10 at Mach 3.0 (Continued).

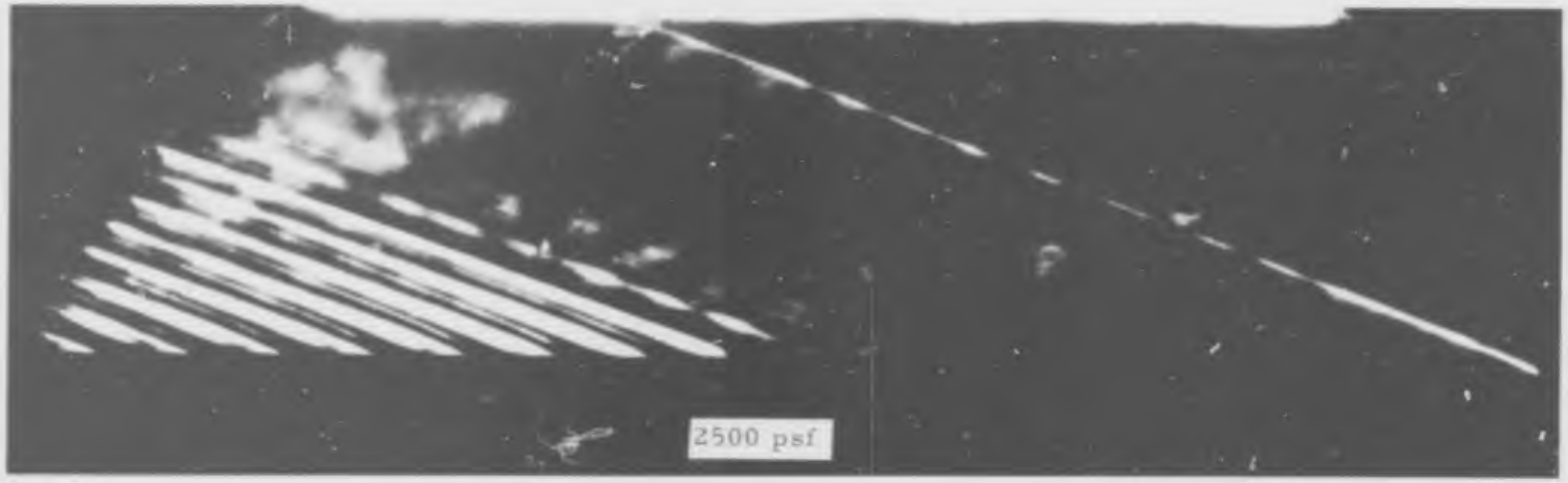

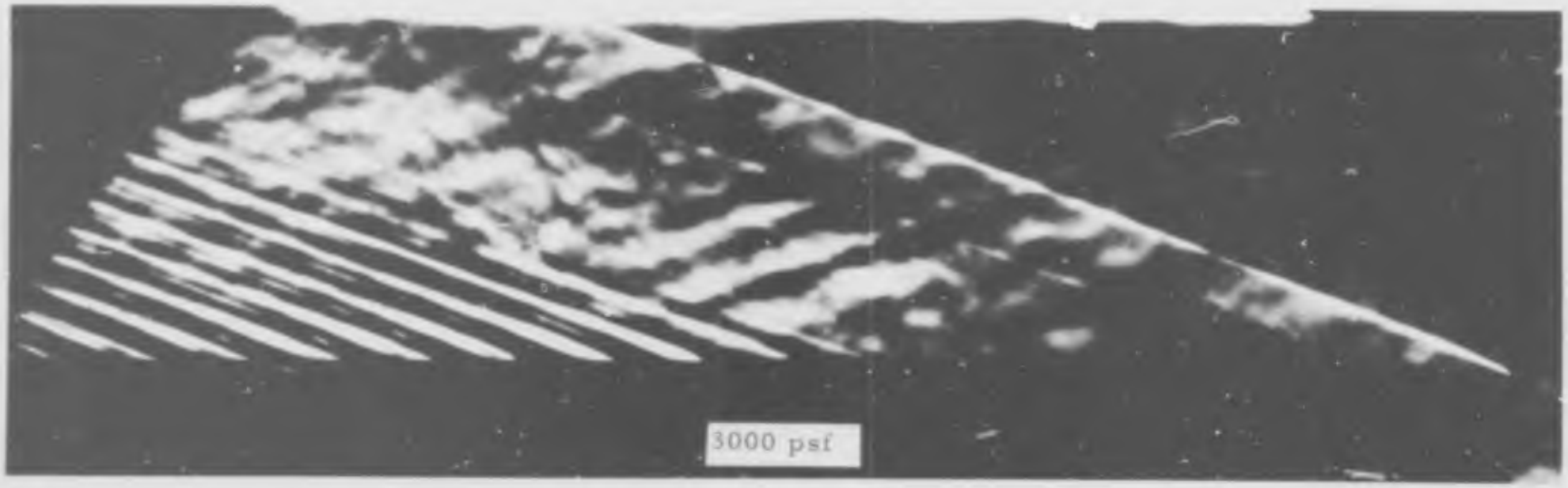

Fig. 19c Shock Pattern on Model #20 at Mach 3.0 (Continued).

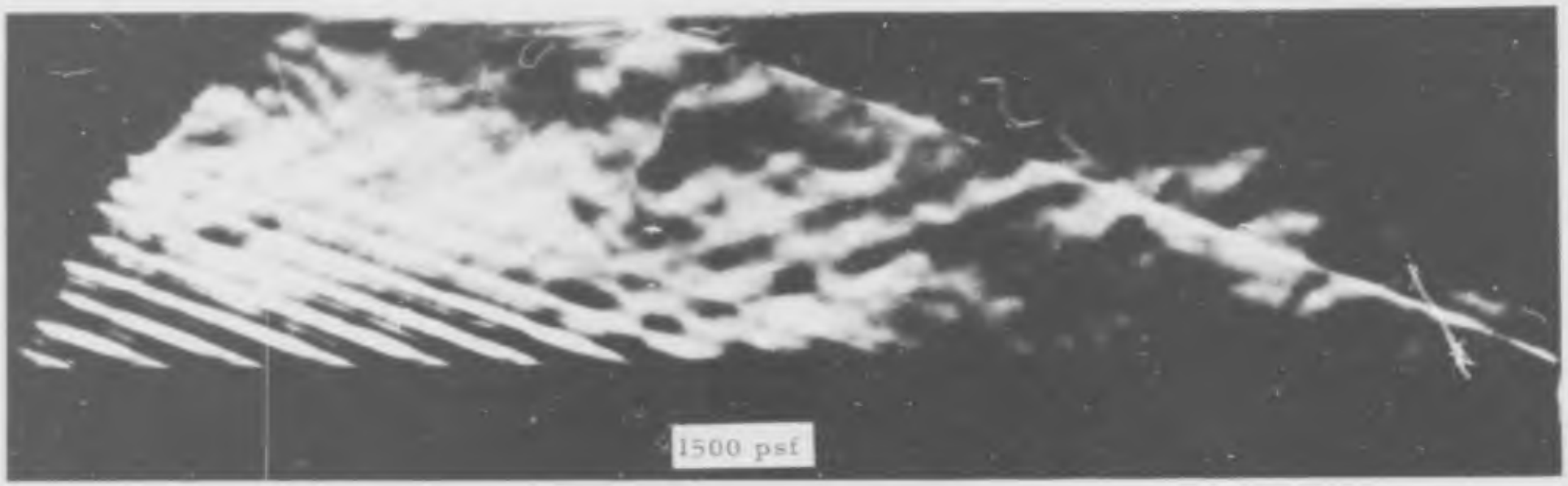

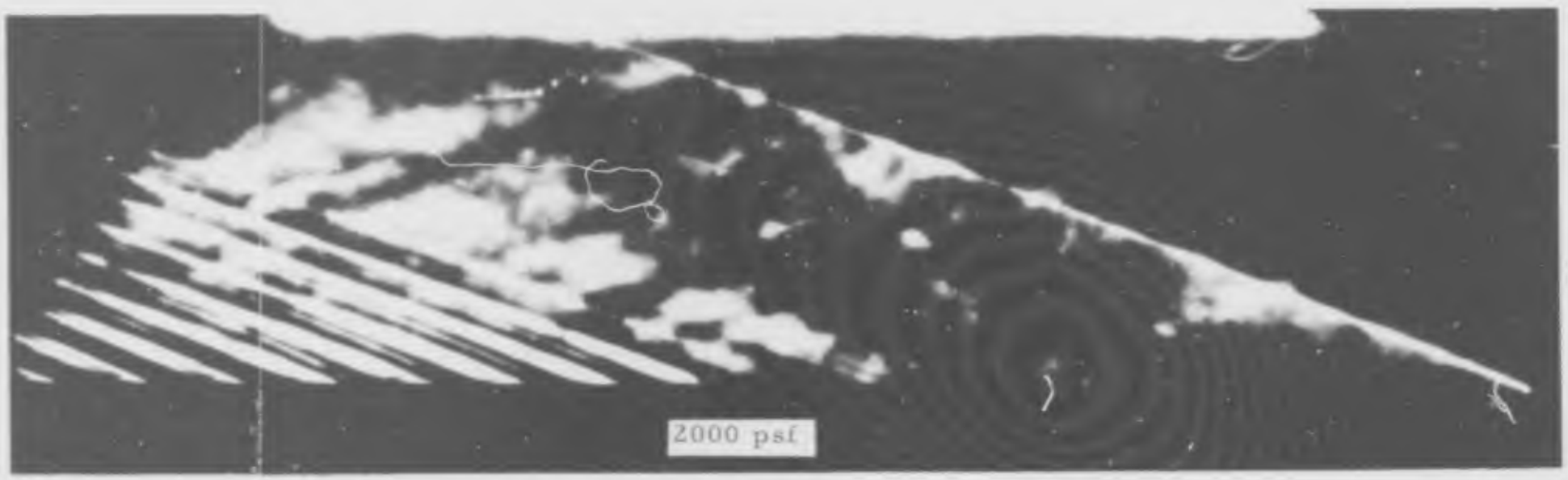

Fig. 19b Shock Pattern on Model #20 at Mach 3.0 (Continued).

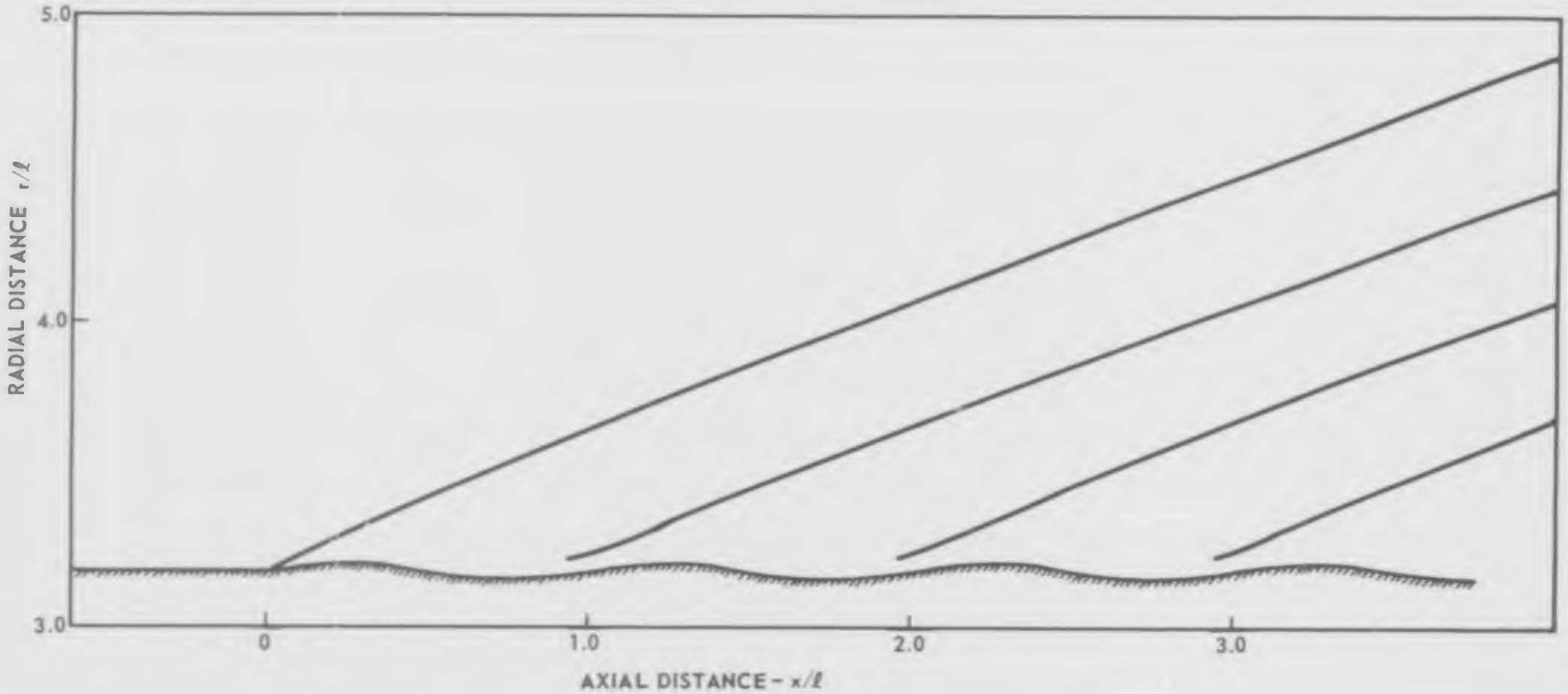

Fig. 21 Theoretical Shock Pattern on Model #0 at Mach 3.0
(Calculations by Saunders, Ref 23)

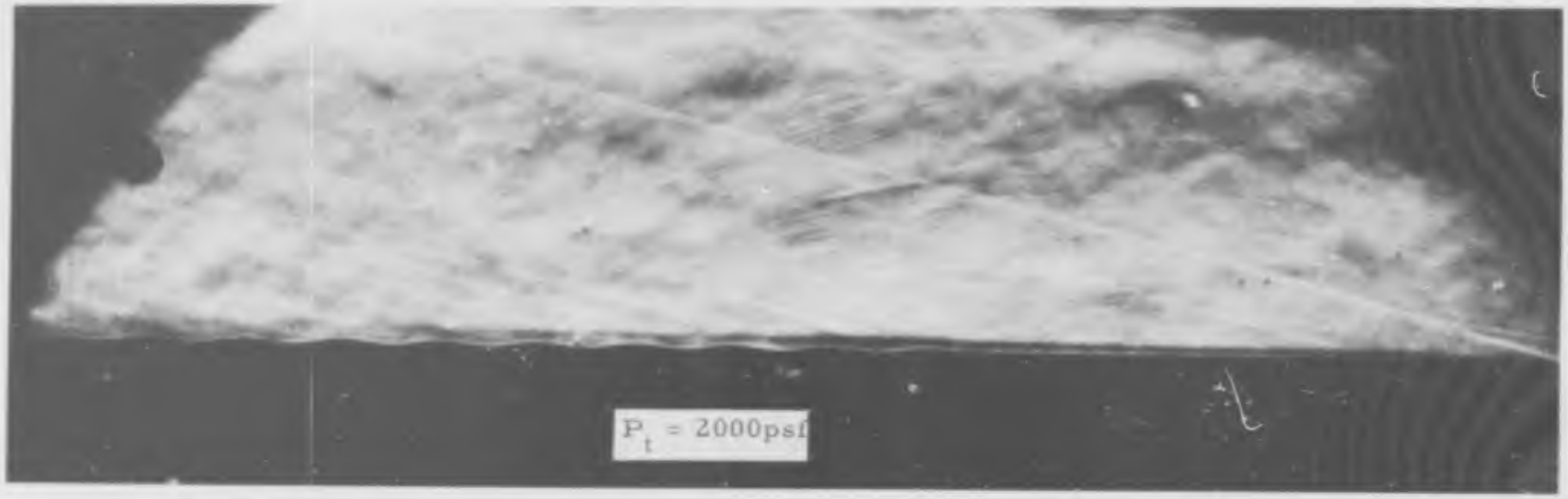

Fig. 20 Shock Pattern on Model #10 at Mach 4.62.

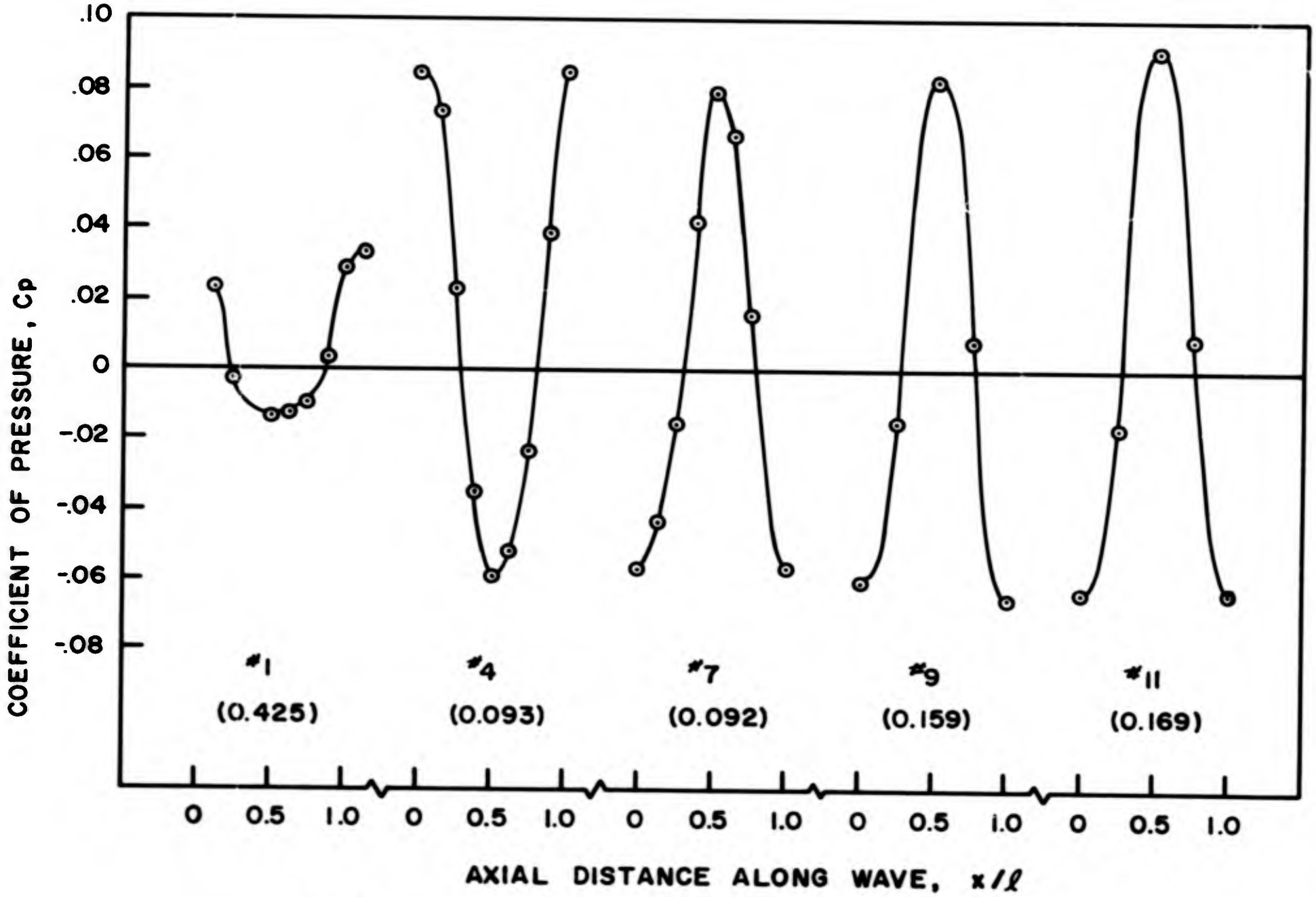

Fig. 23 Static Pressures on Model #10. Mach 3.0, P_t - 2500 psf.

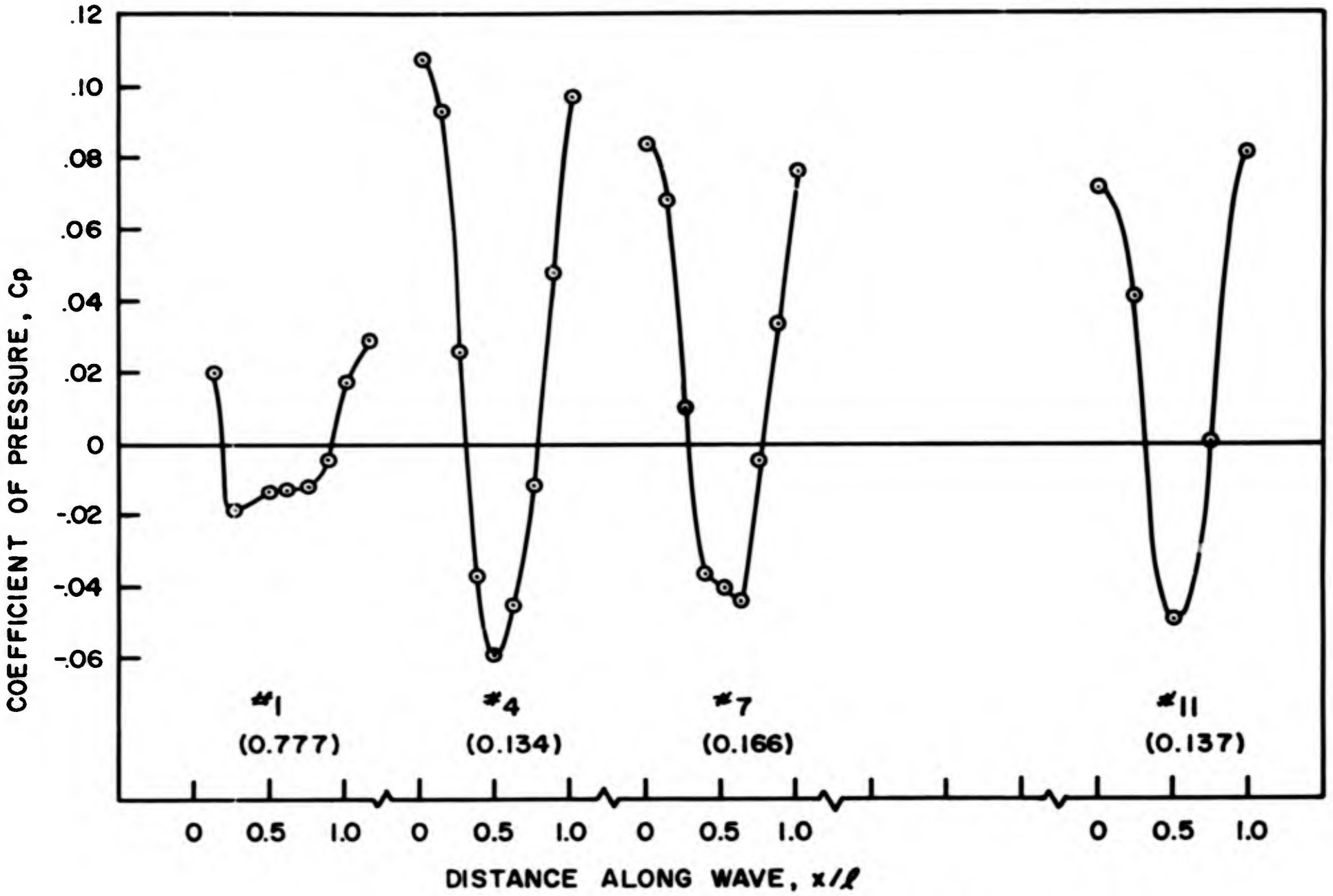

Fig. 22 Static Pressures on Model #0. Mach 3.0, P_t = 2000 psf.

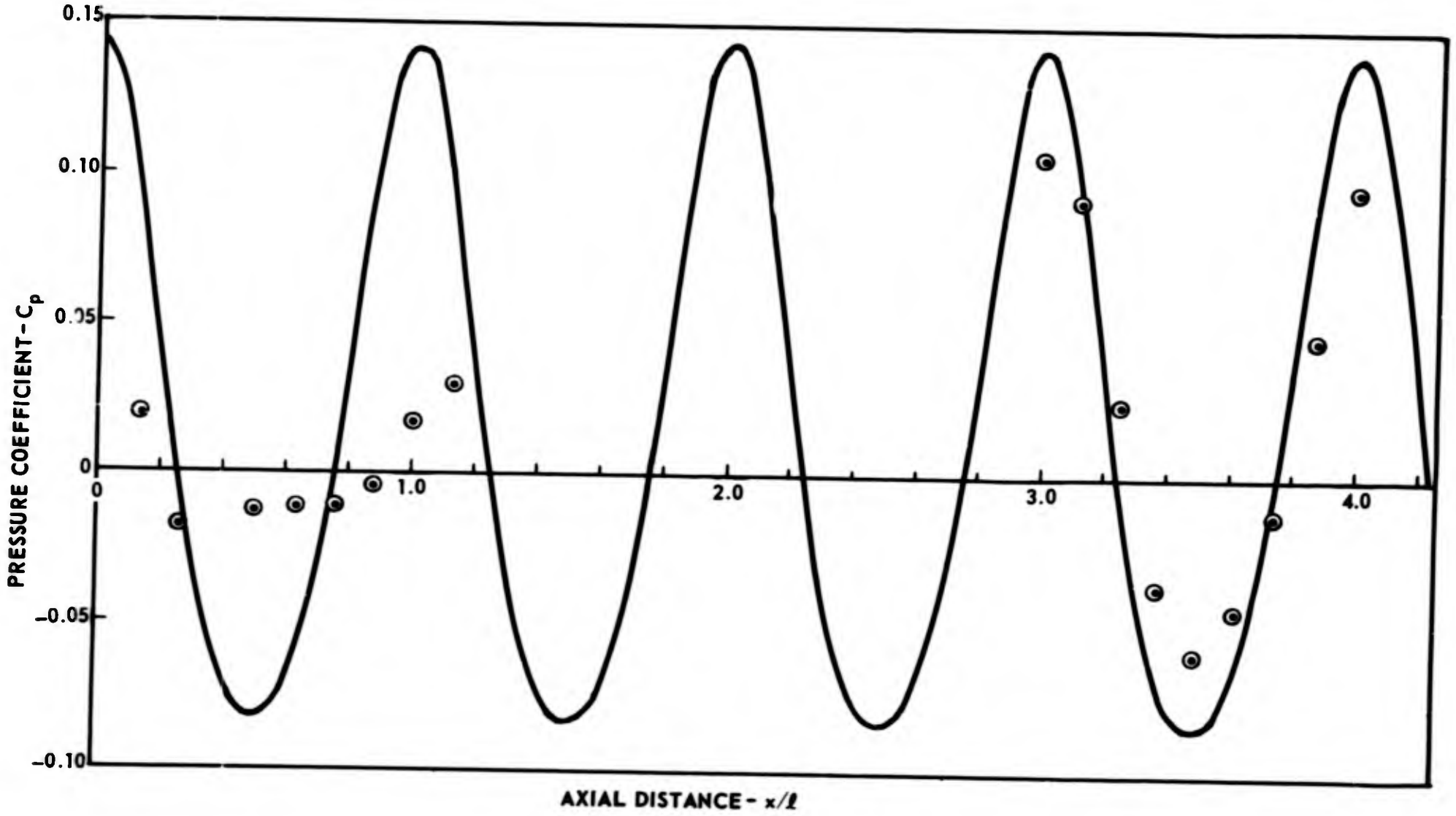

Fig.25a Static Pressures Predicted by Method of Characteristics Solution[23].
(The Experimental Points Shown Here are Taken From Fig. 22)

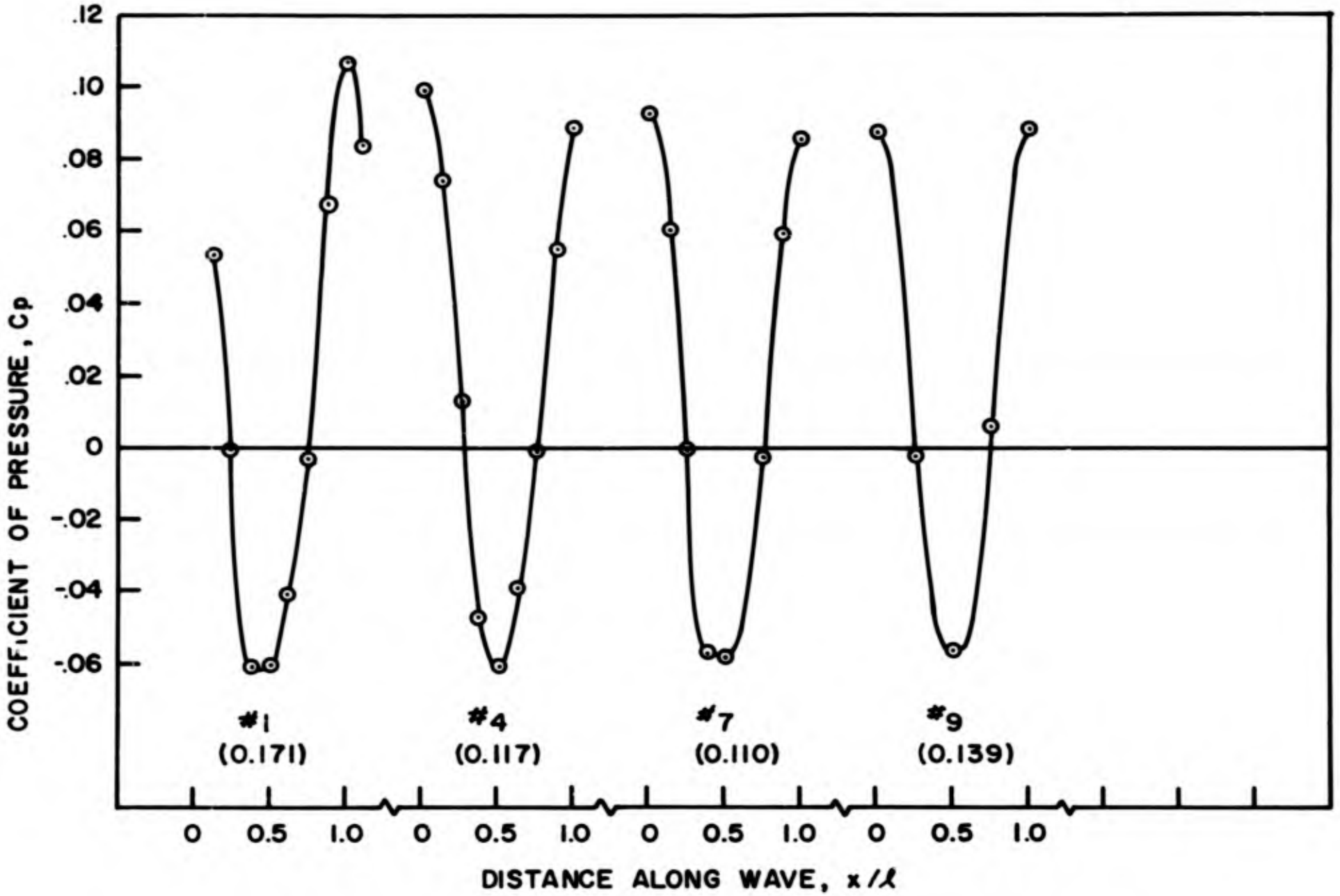

Fig.24 Static Pressures on Model #20 Mach 3.0, P_t = 2500 psf.

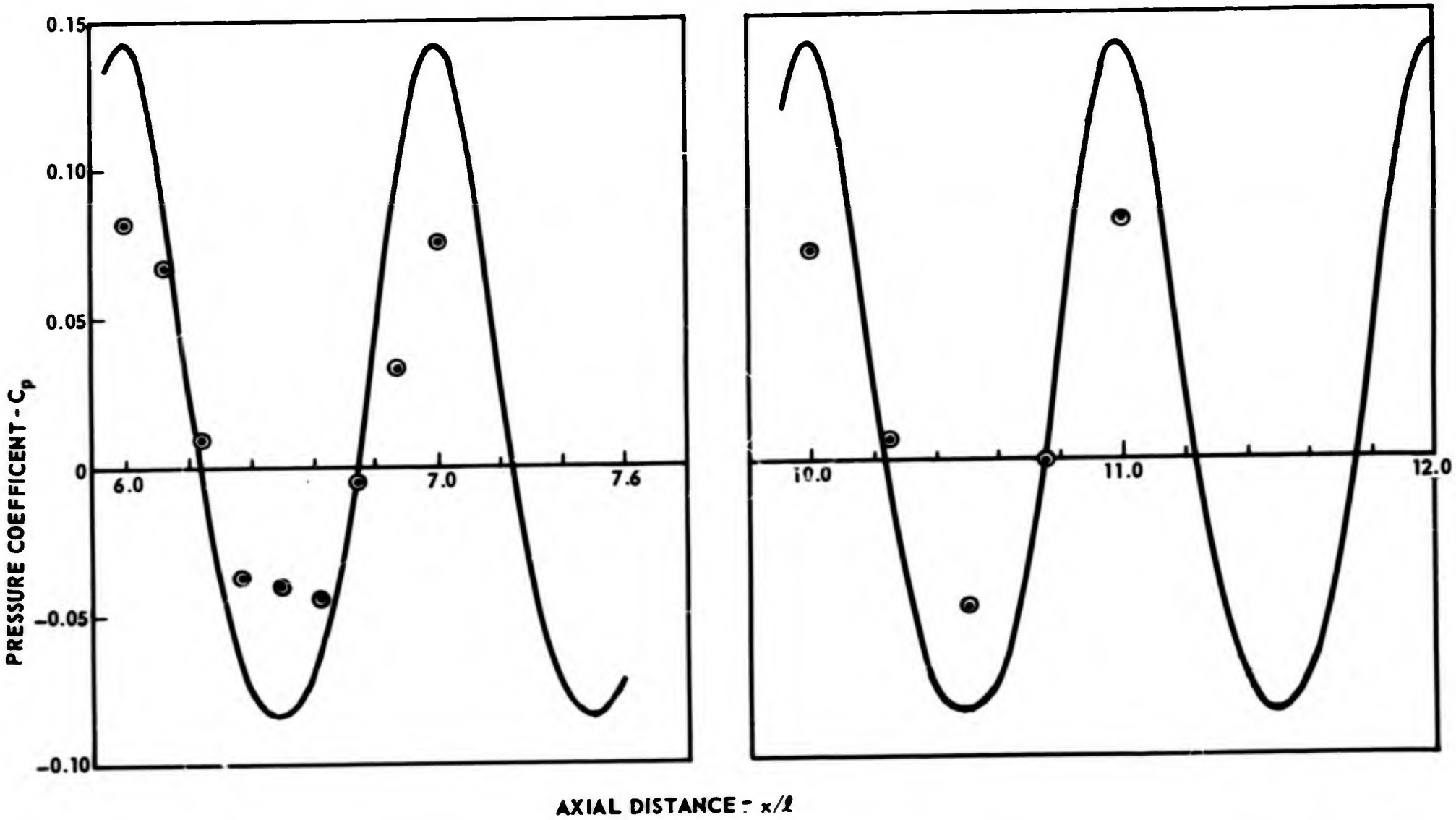

Fig.25b Method of Characteristics Solution (Continued)

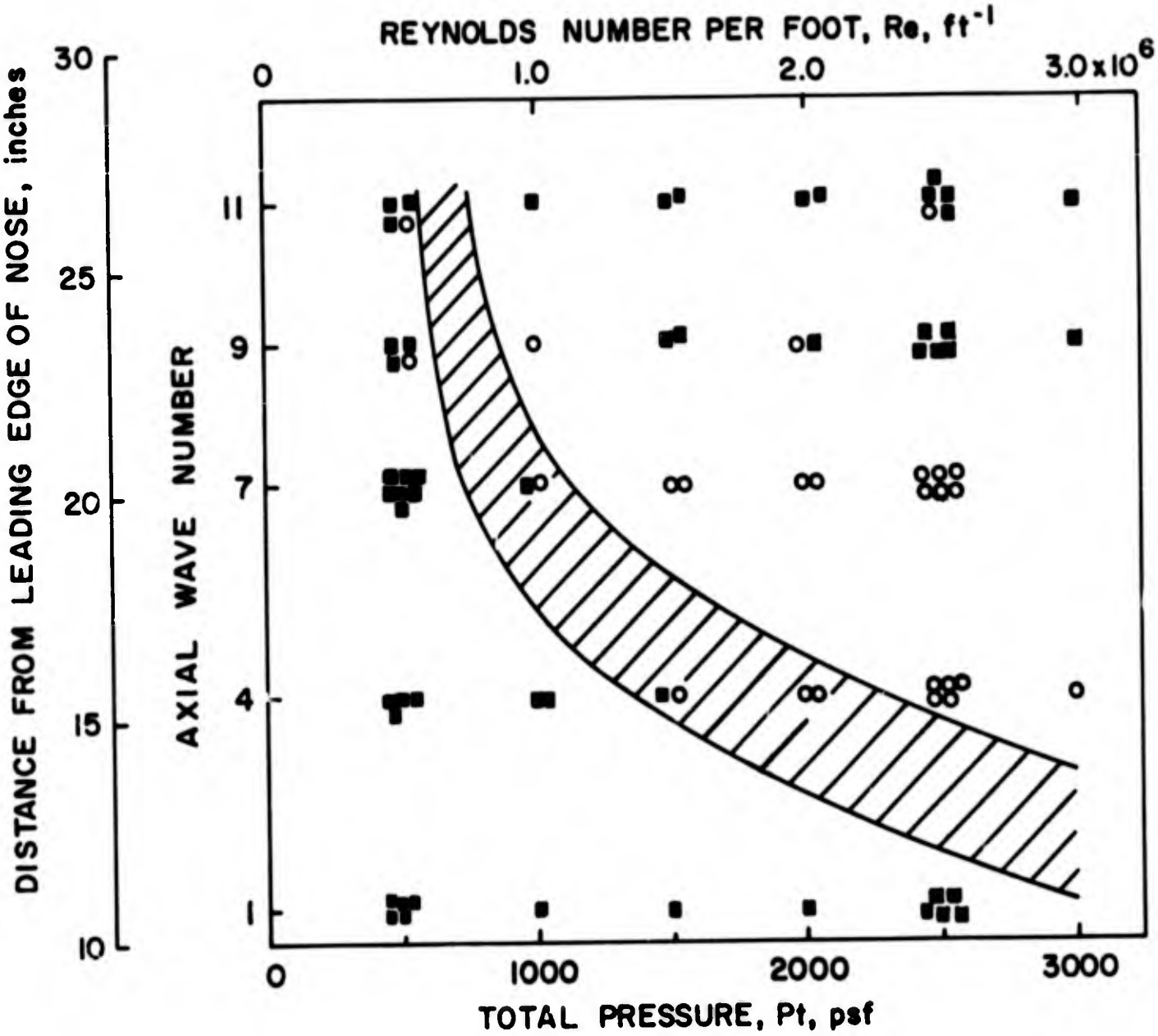

Fig. 26 , Effect of Transition on Boundary Layer Separation (Black Squares Indicate Separated Data. Circles Indicate Unseparated Data. Shaded Area Indicates Boundary Layer Transition Region as Determined by Schlieren Picutres.)

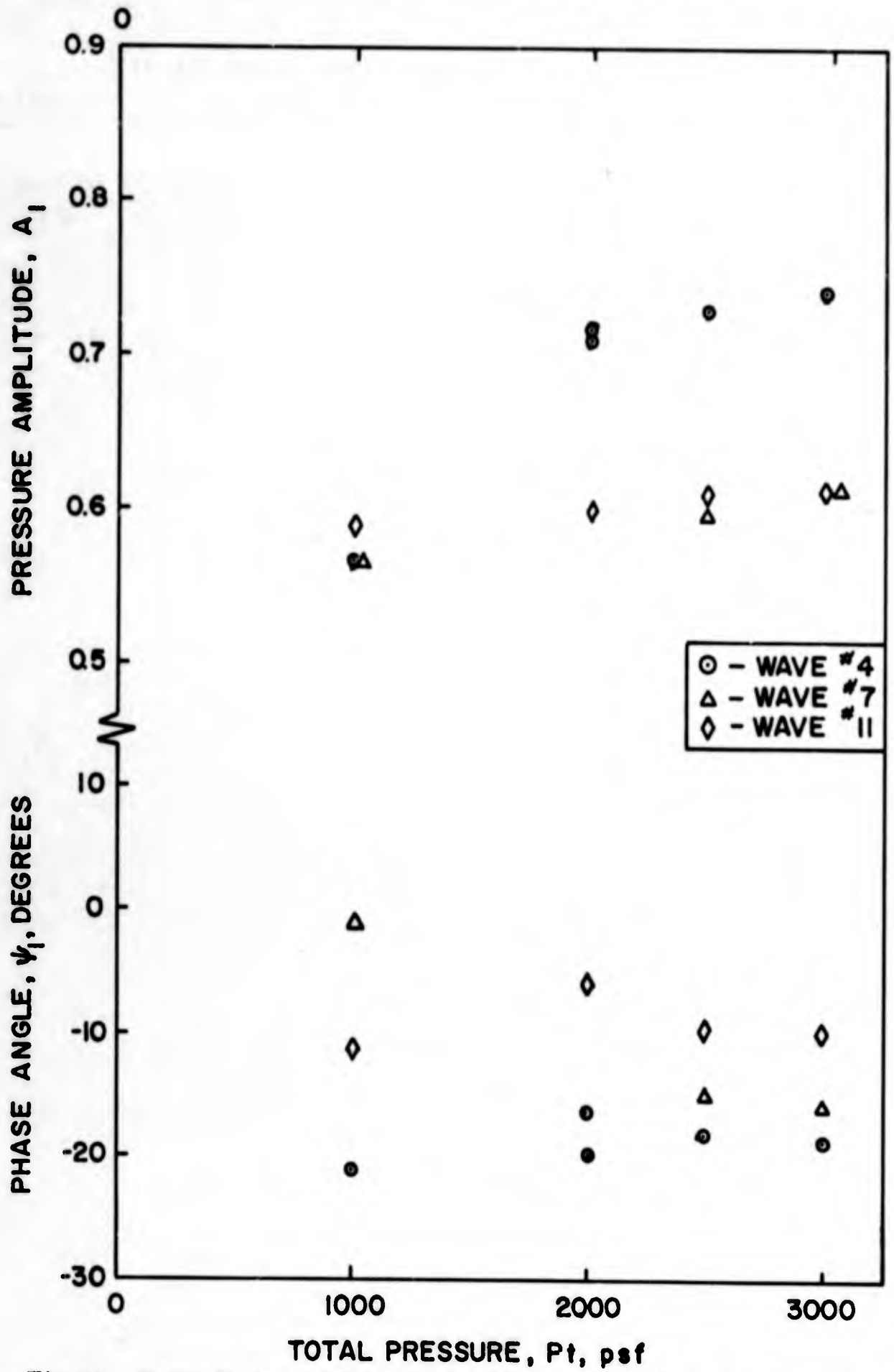

Fig.27 Static Pressure Results for Modei #0 at Mach 3.0 (For These Results, $0.125 \leq E \leq .152$).

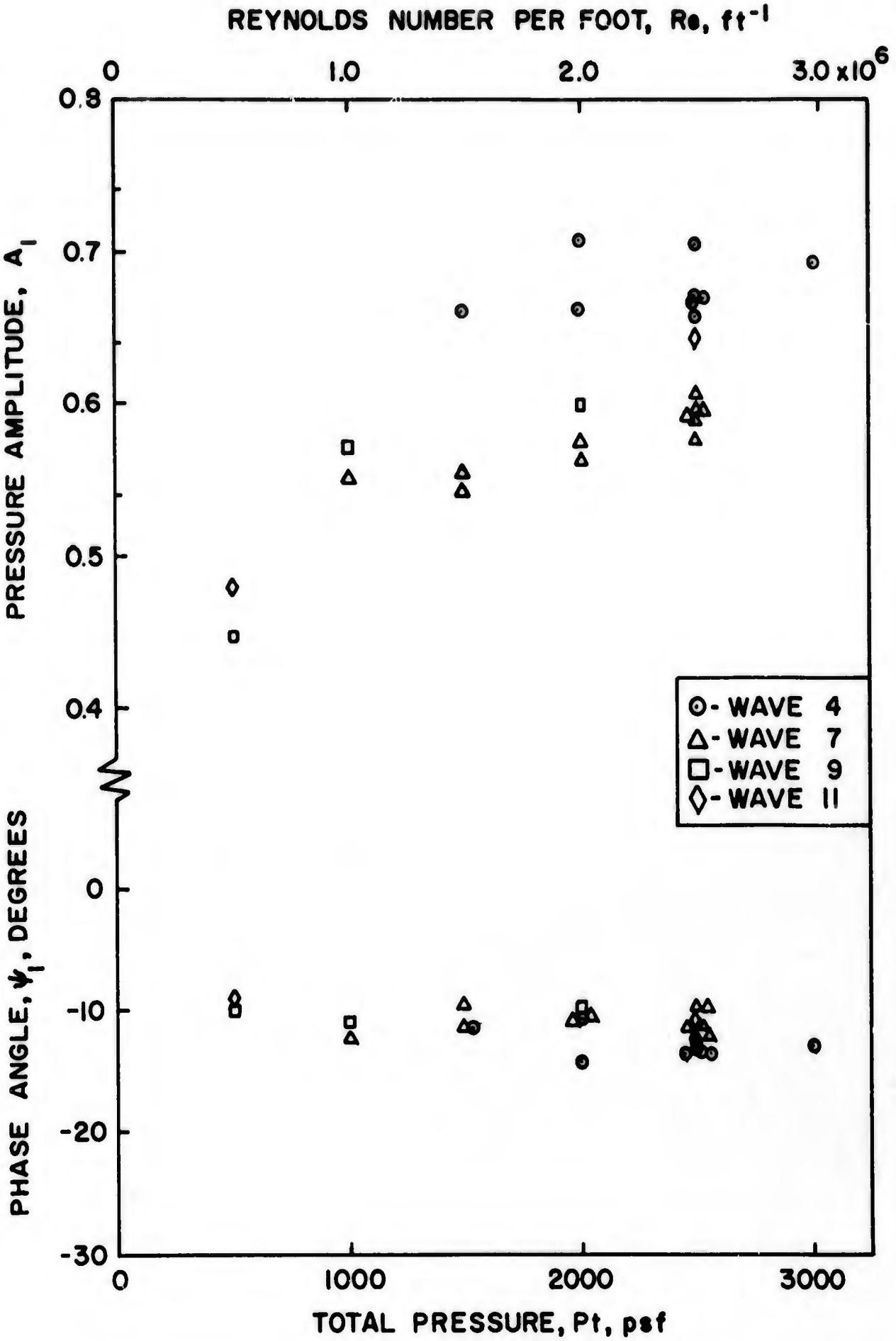

Fig.28 Static Pressure Results for Model #10 at Mach 3.0 (E ≤ 0.125).

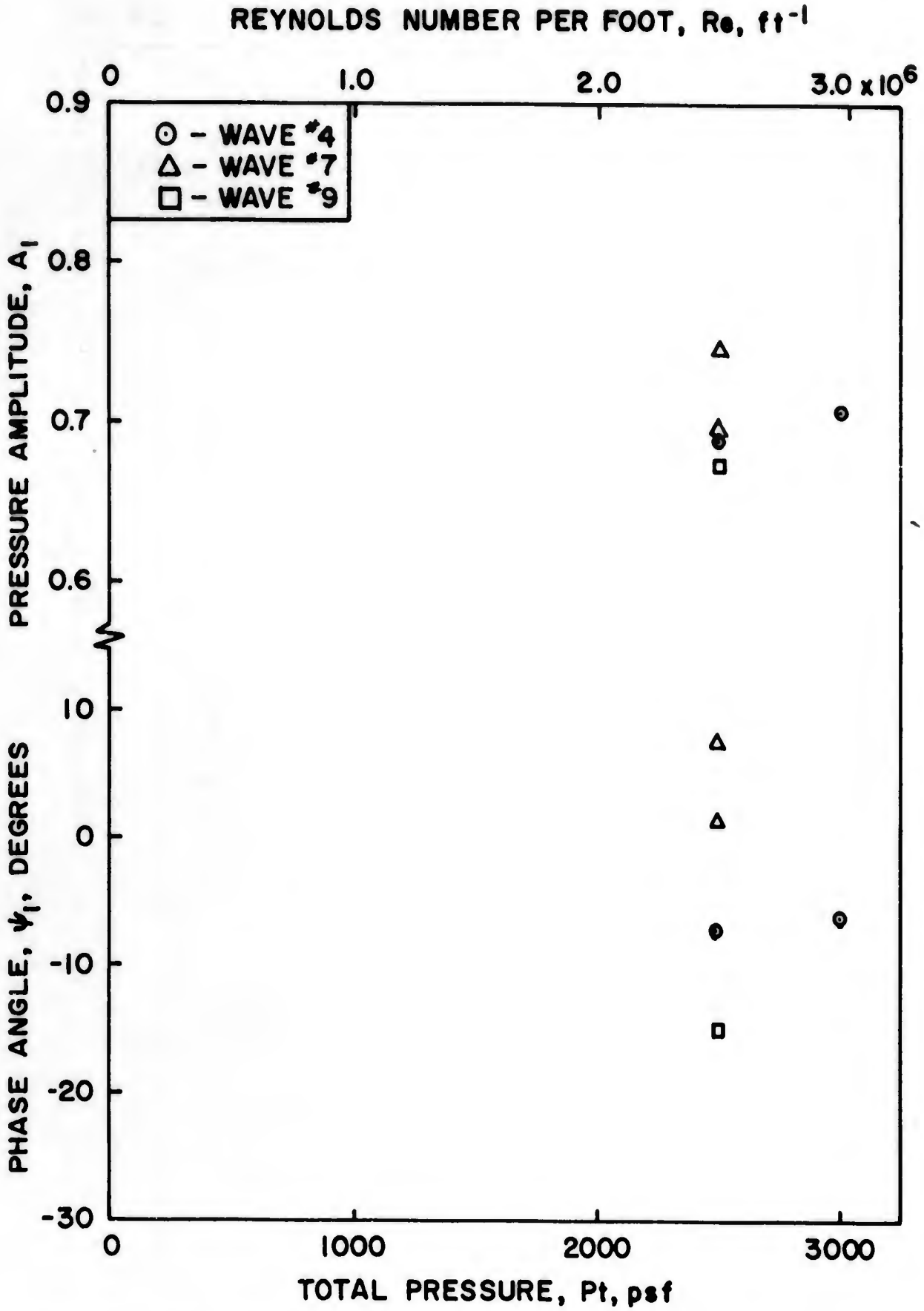

Fig. 29 Static Pressure Results for Model #20 at Mach 3.0 ($E \leq 0.125$).

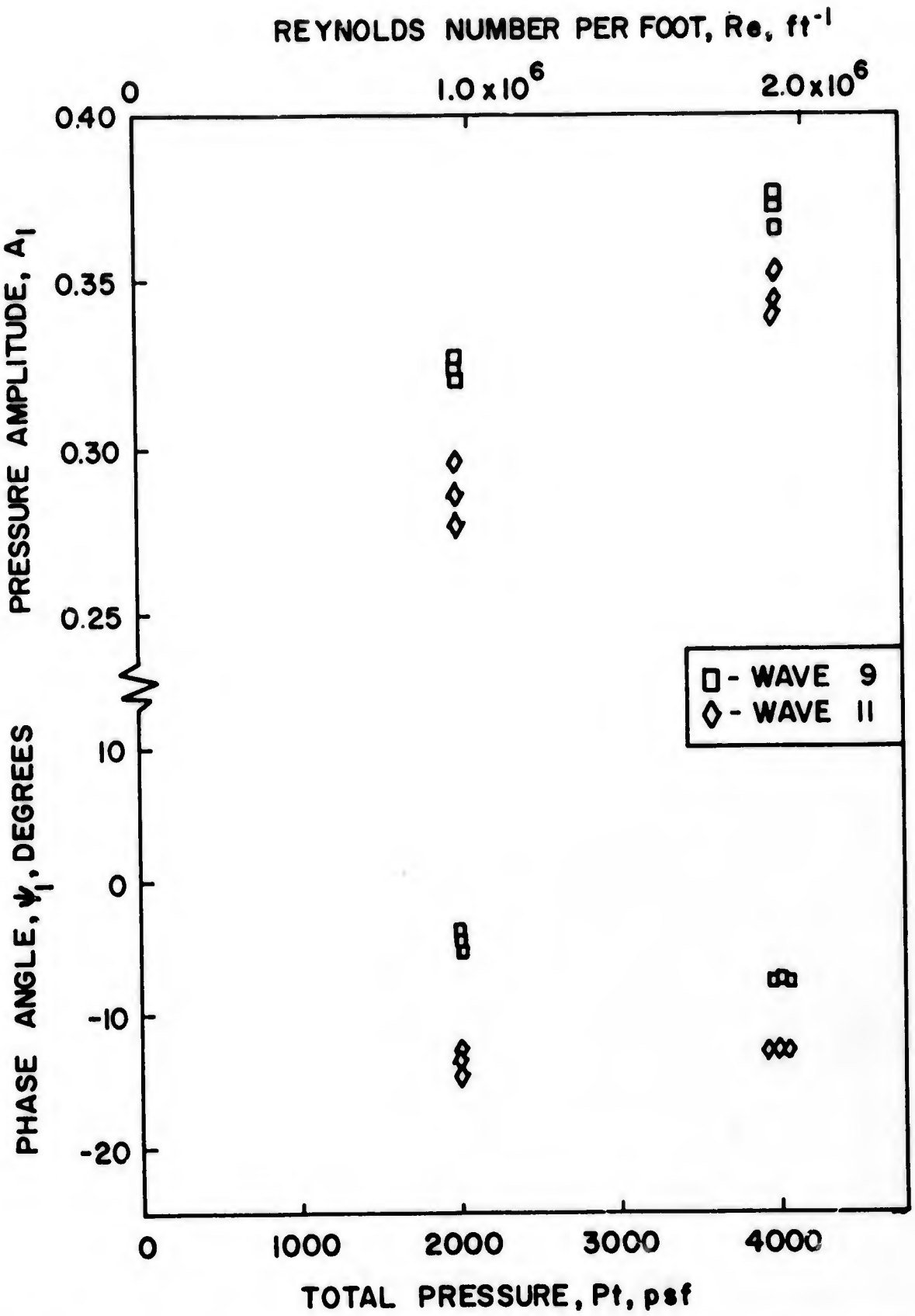

Fig. 30 Static Pressure Results for Model #10 at Mach 4.62 ($E \leq 0.125$).

BLANK PAGE

Unclassified

Security Classification

DOCUMENT CONTROL DATA - R&D

(Security classification of title, body of abstract and indexing annotation must be entered when the overall report is classified)

1. ORIGINATING ACTIVITY *(Corporate author)*

ARL (ARN)

2a. REPORT SECURITY CLASSIFICATION

Unclassified

2b GROUP

3. REPORT TITLE

Supersonic Wind Tunnel Tests of Wavy-Walled Cylinders

4. DESCRIPTIVE NOTES *(Type of report and inclusive dates)*

Final Feb 1964 to April 1964

5. AUTHOR(S) *(Last name, first name, initial)*

Anderson, William J.

6. REPORT DATE	7a. TOTAL NO. OF PAGES	7b. NO. OF REFS
October 1965	59	24

8a. CONTRACT OR GRANT NO.	9a. ORIGINATOR'S REPORT NUMBER(S)
b. PROJECT NO. 7063	
c. 7063-02	9b. OTHER REPORT NO(S) *(Any other numbers that may be assigned this report)*
d.	ARL 65-203

10. AVAILABILITY/LIMITATION NOTICES

Qualified requesters may obtain copies of this report from DDC.
Released to OTS

11. SUPPLEMENTARY NOTES	12. SPONSORING MILITARY ACTIVITY
	ARL-ARN Wright-Patterson AFB, Ohio

13. ABSTRACT The primary objective of this experiment was to provide pressure measurements for use in flutter calculations. Wavy-walled cylinders were wind tunnel tested at Mach 3.0 and 4.62. The walls of the cylinders were rigid, with a sinusoidal deflection pattern machined in the outer surface. The waves extended in both the axial and circumferential direction. Flow was directed along the cylinder axis. Static pressures were measured at the wavy surface of each cylinder. The pressure perturbations proved to be smaller in amplitude than predicted by inviscid aerodynamic theories. The pressure distribution also had a small phase shift downstream. The tests are helpful in studying boundary layer effects on the pressures. The results suggest a choice for an arbitrary parameter appearing in an existing boundary layer theory. A direct comparison with this idealized boundary layer theory was impossible, however, because of the choice of wave height on the model. Qualitative observations also were made concerning the flow over the cylinders. Boundary layer separation occurred under some conditions. In regions on the models where the boundary layer was laminar, separation was observed in the form of a small bubble lying behind a wave. Oil film studies were made by using a thin film of oil on the surface. When exposed to ultraviolet light, the oil film fluoresced, revealing the stream line pattern. Photographs of the oil film patterns and a number of Schlieren pictures are presented. Some details are given pertaining to the model fabrication because of the new manufacturing processes used.

DD FORM 1 JAN 64 1473

Unclassified

Security Classification

Unclassified

Security Classification

14. KEY WORDS	LINK A		LINK B		LINK C	
	ROLE	WT	ROLE	WT	ROLE	WT
Supersonic Wavy-Walled Cylinder Tests, Cylinder Shell Flutter						

INSTRUCTIONS

1. ORIGINATING ACTIVITY: Enter the name and address of the contractor, subcontractor, grantee, Department of Defense activity or other organization *(corporate author)* issuing the report.

2a. REPORT SECURITY CLASSIFICATION: Enter the overall security classification of the report. Indicate whether "Restricted Data" is included. Marking is to be in accordance with appropriate security regulations.

2b. GROUP: Automatic downgrading is specified in DoD Directive 5200.10 and Armed Forces Industrial Manual. Enter the group number. Also, when applicable, show that optional markings have been used for Group 3 and Group 4 as authorized.

3. REPORT TITLE: Enter the complete report title in all capital letters. Titles in all cases should be unclassified. If a meaningful title cannot be selected without classification, show title classification in all capitals in parenthesis immediately following the title.

4. DESCRIPTIVE NOTES: If appropriate, enter the type of report, e.g., interim, progress, summary, annual, or final. Give the inclusive dates when a specific reporting period is covered.

5. AUTHOR(S): Enter the name(s) of author(s) as shown on or in the report. Enter last name, first name, middle initial. If military, show rank and branch of service. The name of the principal author is an absolute minimum requirement.

6. REPORT DATE: Enter the date of the report as day, month, year, or month, year. If more than one date appears on the report, use date of publication.

7a. TOTAL NUMBER OF PAGES: The total page count should follow normal pagination procedures, i.e., enter the number of pages containing information.

7b. NUMBER OF REFERENCES: Enter the total number of references cited in the report.

8a. CONTRACT OR GRANT NUMBER: If appropriate, enter the applicable number of the contract or grant under which the report was written.

8b, 8c, & 8d. PROJECT NUMBER: Enter the appropriate military department identification, such as project number, subproject number, system numbers, task number, etc.

9a. ORIGINATOR'S REPORT NUMBER(S): Enter the official report number by which the document will be identified and controlled by the originating activity. This number must be unique to this report.

9b. OTHER REPORT NUMBER(S): If the report has been assigned any other report numbers *(either by the originator or by the sponsor)*, also enter this number(s).

10. AVAILABILITY/LIMITATION NOTICES: Enter any limitations on further dissemination of the report, other than those imposed by security classification, using standard statements such as:

(1) "Qualified requesters may obtain copies of this report from DDC."

(2) "Foreign announcement and dissemination of this report by DDC is not authorized."

(3) "U. S. Government agencies may obtain copies of this report directly from DDC. Other qualified DDC users shall request through

_____."

(4) "U. S. military agencies may obtain copies of this report directly from DDC. Other qualified users shall request through

_____."

(5) "All distribution of this report is controlled. Qualified DDC users shall request through

_____."

If the report has been furnished to the Office of Technical Services, Department of Commerce, for sale to the public, indicate this fact and enter the price, if known.

11. SUPPLEMENTARY NOTES: Use for additional explanatory notes.

12. SPONSORING MILITARY ACTIVITY: Enter the name of the departmental project office or laboratory sponsoring *(paying for)* the research and development. Include address.

13. ABSTRACT: Enter an abstract giving a brief and factual summary of the document indicative of the report, even though it may also appear elsewhere in the body of the technical report. If additional space is required, a continuation sheet shall be attached.

It is highly desirable that the abstract of classified reports be unclassified. Each paragraph of the abstract shall end with an indication of the military security classification of the information in the paragraph, represented as *(TS), (S), (C), or (U)*

There is no limitation on the length of the abstract. However, the suggested length is from 150 to 225 words.

14. KEY WORDS: Key words are technically meaningful terms or short phrases that characterize a report and may be used as index entries for cataloging the report. Key words must be selected so that no security classification is required. Identifiers, such as equipment model designation, trade name, military project code name, geographic location, may be used as key words but will be followed by an indication of technical context. The assignment of links, rules, and weights is optional.

Security Classification